Seasonal Prediction Experiments with a Regional Model Nested in a Global Model

M. J. Fennessy and J. Shukla

Center for Ocean-Land-Atmosphere Studies
4041 Powder Mill Road, Suite 302
Calverton, MD 20705

December 1998

Abstract

Ensembles of winter and summer seasonal simulations have been carried out with an 80 km resolution version of the National Centers for Environmental Prediction (NCEP), Environmental Modeling Center (EMC) Eta model over the North American region. The lateral boundary conditions for the Eta model are prescribed from Center for Ocean-Land Atmosphere (COLA) R40 atmospheric general circulation model (AGCM) integrations which used observed atmospheric initial conditions and observed global sea surface temperature (SST).

An examination of 15 seasonal winter simulations and 15 seasonal summer simulations shows that the nested model significantly improves the simulations of seasonal precipitation compared to the global model alone. The physical parameterizations, enhanced resolution and better representation of orography in the Eta model produce better simulations of precipitation and its interannual variability. In particular, the precipitation difference between the 1988 drought and 1993 flood over the U.S. was much better simulated by the nested model. The simulations of circulation features were generally as good or better than those from the global model alone.

Estimates of external (SST-forced "signal") and internal (dynamics-generated "noise") variability were made for both the global model and the nested model simulations. Contrary to the expectation that a higher resolution model would have higher internal dynamics-generated variability, the signal, noise and signal-to-noise ratios of the near surface temperature and precipitation fields were generally quite similar between the nested model and the global model simulations. In the winter season, the nested model had larger signal-to-noise ratios in both temperature and precipitation than did the global model alone.

1. Introduction

Research during the past 20 years has established that seasonal climate anomalies over continental regions are forced, in part, by the slowly varying boundary conditions of sea surface temperature (SST) and land surface conditions. It is also well established that SST anomalies, particularly in the tropical oceans, can be predicted by coupled ocean-atmosphere models. It is therefore reasonable to expect that accurate predictions of boundary conditions would allow prediction of regional climate anomalies for lead times beyond the limit of deterministic predictability (Shukla, 1998). However, the current atmospheric general circulations models (AGCMs) are unable to accurately simulate the regional precipitation anomalies over the continents even with prescribed observed global SST anomalies. Is this inability to simulate regional precipitation a fundamental constraint of the predictability of the regional climate or is it due to the parameterizations and spatial resolution of the current AGCMs? The current AGCMs do not have sufficient horizontal resolution to resolve regional orographically-forced precipitation features and a systematic study with a very high resolution global AGCM to address this question would require more computer time than is currently available.

An alternative approach to address this question which requires less computing time is outlined schematically in the upper left half of Fig. 1. At the upper left corner of the diagram, the low resolution coupled ocean-land-atmosphere model is used to predict the anomalous surface boundary conditions of SST, soil wetness, and snow depth which are the most important determinants of predictable seasonal to interannual climate variations. The predicted boundary conditions are then applied to a medium resolution global atmospheric

model that is integrated for a season to produce the global circulation and planetary scale waves that occur in response to the anomalous boundary conditions. A limited area high resolution atmospheric model is then nested in the global atmospheric model by applying the global circulation predicted by the medium resolution model as a lateral boundary condition to the high resolution regional model. Given a sufficiently large domain for the nested model, this matching at the boundaries only specifies the continental scale heat and moisture flux divergences and allows the distribution of temperature and precipitation within the domain to be significantly different from that of the global model. The regional climatic details that are indistinct or even erroneous in the medium resolution model could be more skillfully predicted by the high resolution model. This procedure allows us to address the following question: Can the predictable component of the large scale atmospheric circulation be used in conjunction with high resolution regional dynamical models to predict regional climate in North America at seasonal and longer lead times? Results of Giorgi and Bates (1989) and Giorgi (1990) for the western U. S., Ji (1996) and Ji and Vernekar (1997) for the Indian monsoon region, and Tanajura (1996) for the South American region, among others, have already provided strong evidence for scientific justification of this procedure. This paper presents a test of this procedure for North American regional climate. If this procedure is successful, the output of the high resolution regional model could then be used to drive hydrology, water management and socio-economic policy models (Fig. 1, lower right half).

Because the lead time of interest is longer than the inherent limit of deterministic predictability of instantaneous atmospheric flows, an element of uncertainty is present at

each step of the procedure described by Fig. 1. In order to make the predictions more robust and to quantify the uncertainty, it is necessary to make multiple realizations with each model. The multiple realizations are produced by perturbing the initial conditions used in each model and repeating the model integration with each of the perturbed initial states.

An 80 km version of the National Centers for Environmental Prediction (NCEP) Environmental Modeling Center (EMC) Eta model (Black, 1994), centered over North America was nested in the COLA R40 global AGCM for seasonal integrations. The Eta model was chosen following the successful results of Ji and Vernekar (1997), in simulating seasonal mean features and interannual variability of the Indian summer monsoon rainfall and Tanajura (1996), in simulating the South American climate, both using the Eta model. In this hindcast experiment, both models were integrated with the same time-varying observed weekly SST (Reynolds and Smith, 1994) as the lower boundary condition. Otherwise, the AGCM was provided no additional input after initialization and the nested Eta regional model was provided only the lateral boundary conditions from the AGCM at 12-hour intervals. The frequency of the lateral boundary updating was determined by the availability of AGCM output from existing integrations. Ensembles of three nested integrations for each of five different years were performed and compared with observations and with integrations of the AGCM alone.

The model formulations and experimental design are described in Section 2. The seasonal mean climate simulations are presented in Section 3. Aspects of the simulation of the observed interannual variability, including systematic and root mean square errors, are discussed in Section 4. Signal-to-noise calculations are presented in Section 5.

Conclusions and further work required are discussed in Section 6.

2. Models and experimental design

a. COLA AGCM

The COLA AGCM is based on a modified version of the NCEP global spectral model used for medium range weather forecasting (see Sela, 1980 for original NCEP formulation; see Kinter et al., 1988, 1997 and DeWitt, 1996 for the modified version). The land surface parameterization was changed to the Simple Biosphere model (SiB) biophysical formulation after Sellers et al. (1986) by Sato et al. (1989) and later simplified by Xue et al. (1991). The model includes the relaxed Arakawa-Schubert convection (Moorthi and Suarez, 1992; after Arakawa and Schubert, 1974), and the Tiedtke (1984) shallow convection after Hogan and Rosemond, (1991), both described by DeWitt (1996).

The COLA AGCM is a global spectral model with rhomboidal truncation at zonal wave number 40 (R40). The parameterization calculations are done on a 1.8° latitude by 2.8° longitude Gaussian grid. The vertical structure of the model is represented by 18 unevenly spaced levels using σ as the vertical coordinate (Phillips, 1957). The spacing of the levels is such that greater resolution is obtained near the Earth's surface and at the tropopause. In addition to the parameterizations mentioned above, the COLA AGCM includes parameterizations of solar radiative heating (Lacis and Hansen, 1974), terrestrial radiative heating (Harshvardhan et al., 1987), large scale condensation, interactive cloud-radiation (Hou, 1990; after Slingo, 1987), gravity wave drag (Vernekar et al., 1992; after Alpert et al., 1988) and a turbulence closure scheme for subgrid scale exchanges of heat,

momentum and moisture (Miyakoda and Sirutis, 1977; Mellor and Yamada, 1982).

In the COLA AGCM, each land grid box is assigned one of twelve sets of vegetation and soil characteristics, based on the dominant vegetation observed in the grid box (Dorman and Sellers; 1989, Fennessy and Xue, 1997). Included in these characteristics are the depth and porosity of each of three soil layers: the surface layer, the root zone and the drainage layer. The total depth of the three layers ranges from 0.49 m for bare soil (desert) to 3.5 m for trees. The total water holding capacity ranges from 0.21 m for bare soil to 1.47 m for trees. The soil wetness is initialized from proxy seasonally varying soil wetness derived from data produced by the ECMWF analysis-forecast system (Fennessy and Shukla, 1996). The model uses mean orography calculated from the U.S. Navy 10 minute elevation data.

b. NCEP EMC Eta regional model

The regional model used in this study is a slightly modified version of the NCEP EMC Eta model that became operational in March 1997. For the sake of computational efficiency, the horizontal resolution was reduced from 48 km to 80 km (as used operationally until October, 1995). Aside from changing the horizontal resolution, the model is almost identical to the operational version which is routinely run for 48 hours, except for procedural changes[1] which were necessary to make longer climate integrations and to nest the model in the COLA R40 AGCM. The 80 km regional model integration domain used here (92x141 grid, Fig. 2, heavy line) is nearly identical to the "early" Eta 48 km domain used operationally in March 1997 (160x261 grid, Fig. 2, light line).

---

[1]The Eta model physics and dynamics were not altered. Minor code changes were necessary to run the model longer than 48 hours (timekeeping, data set updates, etc.) and to use the different format/resolution COLA AGCM lateral boundary conditions.

The Eta model is a state-of-the-art mesoscale weather forecast model with an accurate treatment of complex topography using the eta vertical coordinate and steplike mountains (Mesinger ,1984), which eliminates the errors in the pressure gradient force over steeply sloped terrain present in sigma coordinates (Mesinger and Black, 1992). The recent version used here follows that described by Mesinger et al., 1988; Black, 1994 and Rogers et al., 1995, 1996; and Mesinger, 1996). The model employs a semistaggered Arakawa E-grid in which wind points are adjacent to mass points (Arakawa and Lamb, 1977), configured in rotated spherical coordinates. There are 38 Eta vertical levels and the model top is at 50 mb. Split-explicit time differencing is used with a 120-second adjustment time step. Space differencing is done with a conserving Arakawa-type scheme (Janic, 1984). The eta steplike mountains are derived from the silhouette-mean orography of Mesinger (1995). The orography used in the COLA AGCM, the nested Eta model and their difference is shown in Fig. 3a-3c respectively. Large differences of up to 500 m or more occur in the vicinity of the Sierra Nevada, the Rocky and the Appalachian Mountains. In particular, the latter are present in the Eta orography (Fig. 3b) and all but absent in the COLA AGCM orography (Fig. 3a).

The model physics has been described by Janjic (1990, 1994) and includes a modified Betts-Miller scheme for deep and shallow convection (Betts and Miller, 1986; Janjic, 1994), and predicted cloud water/ice (Zhao et al., 1997). The GFDL scheme is used for radiation (Fels and Schwarzkopf, 1975; Lacis and Hansen, 1974). Free atmospheric turbulent exchange above the lowest model layer is computed using a Mellor-Yamada (1982) level-2.5 closure and the surface layer similarity functions are derived from Mellor-Yamada level-2.0

closure (Lobocki, 1993). A viscous sublayer is used over water surfaces (Janjic, 1994). The land surface is a version of the OSU scheme modified by Chen et al., (1997).

c. Experimental design

The COLA AGCM integrations were done first and data were saved every 12 hours. For each of the COLA AGCM integrations, a nested integration with the Eta model was done, starting from the same initial date and initial data as the AGCM and using as lateral boundary conditions the 12-hourly AGCM data linearly interpolated in time. This one-way nesting technique is similar to that used by Ji and Vernekar (1997), and it includes a 2 grid-point overlap as used operationally at NCEP.

The 15 summer integrations were initialized in late May and span all of June, July, August and September. The fifteen winter integrations were initialized in mid-December and span all of January, February and March. All the integrations were initialized from analyses of the observations, either from the National Meteorological Center (NMC) operational analyses, the National Center for Environmental Prediction (NCEP) reanalyses or the COLA reanalyses. The integration initial dates and initialization data sources are given in Table 1. The years were chosen from a set of pre-existing COLA AGCM integrations. This choice favored selection of ENSO years and years with interesting North American climate anomalies.

Summer Integrations		Winter Integrations	
00UTC 29 May 1986	NCEP Reanalysis	00UTC 13 Dec 1982	COLA Reanalysis
00UTC 30 May 1986	NCEP Reanalysis	12UTC 13 Dec 1982	COLA Reanalysis
00UTC 31 May 1986	NCEP Reanalysis	00UTC 14 Dec 1982	COLA Reanalysis
00UTC 28 May 1987	NMC Analysis	00UTC 13 Dec 1984	NCEP Reanalysis
12UTC 28 May 1987	NMC Analysis	12UTC 13 Dec 1984	NCEP Reanalysis
00UTC 29 May 1987	NMC Analysis	00UTC 14 Dec 1984	NCEP Reanalysis
00UTC 28 May 1988	NMC Analysis	00UTC 13 Dec 1986	NMC Analysis
12UTC 28 May 1988	NMC Analysis	12UTC 13 Dec 1986	NMC Analysis
12UTC 30 May 1988	NMC Analysis	12UTC 14 Dec 1986	NMC Analysis
00UTC 28 May 1993	NMC Analysis	00UTC 13 Dec 1988	NCEP Reanalysis
12UTC 28 May 1993	NMC Analysis	12UTC 13 Dec 1988	NCEP Reanalysis
00UTC 29 May 1993	NMC Analysis	00UTC 14 Dec 1988	NCEP Reanalysis
00UTC 28 May 1994	NMC Analysis	00UTC 13 Dec 1990	NCEP Reanalysis
12UTC 28 May 1994	NMC Analysis	12UTC 13 Dec 1990	NCEP Reanalysis
00UTC 29 May 1994	NMC Analysis	00UTC 14 Dec 1990	NCEP Reanalysis

TABLE 1. Integration initial dates and initialization data sources.

Observed time-varying weekly SST (Reynolds and Smith, 1994) was linearly interpolated in time and used in all the integrations. The soil wetness and snow were predicted after initialization in both the AGCM and the nested Eta model by their respective parameterizations. Because the surface physics treatments in these two models are quite different, the initialization of the snow and soil wetness are not identical, but follow the same

principles.

The snow cover in each model was initialized from seasonally varying climatological data. In the COLA AGCM, the snow is initialized via an algorithm that derives daily snow cover and snow depth from the seasonal albedo data of Posey and Clapp (1954). In the Eta model, the snow is initialized via an algorithm that derives daily snow cover and snow depth from a 1967-1980 daily snow cover climatology calculated from the weekly NESDIS snow/ice mask. The initial snow cover used in the AGCM and the nested Eta model were compared and were found to be quite similar.

All the integrations were initialized with observationally-based soil wetness. The soil wetness used for initialization of the AGCM integrations was derived from the operational ECMWF analysis-forecast cycle soil moisture via an algorithm described by Fennessy and Shukla (1996). The 1987, 1988 and 1993 summer AGCM integrations were initialized with the ECMWF derived soil wetness, and the 1986 and 1994 summer AGCM integrations and all the winter AGCM integrations were initialized with a 1987-1993 climatology of the ECMWF derived soil wetness. The nested Eta integrations were all initialized with NCEP reanalysis soil wetness obtained from the data archived at the National Center for Atmospheric Research (NCAR).

3. Seasonal mean climate simulations

To evaluate how the nested Eta model simulations compare to those from the AGCM alone, 15-member ensemble seasonal means which are composed of three integrations from each of five different years are examined (Table 1). These ensembles are compared to observations averaged over the same five years. All figures show continental

North America and the adjoining ocean areas, which is the main region of interest, rather than the whole domain, which is shown in Fig. 2. For the initial stage of analysis, examination of simulated fields confirmed that the AGCM and nested simulations match at the lateral boundaries.

a. Summer

The five-year mean June-July-August-September (JJAS) two meter temperature obtained from Climate Anomaly Monitoring System (CAMS, Ropelewski et al., 1985) station data is shown in Fig. 4a. The corresponding ensemble mean errors for the AGCM and the nested model are shown in Figs. 4 b,c respectively. The model temperatures are adjusted using a lapse rate of 6.5 °C km^{-1} for the difference between the elevation of each model grid box and the mean elevation of the stations used to form the gridded observation. Both models have significant negative errors of 2 °C or more over much of the continent, but the AGCM errors are larger, reaching 4 °C or more over northern Alaska and Canada. However, the region of 1 °C or more negative error in the nested model covers more of the continent than it does in the AGCM.

The observed five-year mean JJAS precipitation from a combination of station and satellite data (Xie and Arkin, 1996) is shown in Fig. 5a. The corresponding ensemble mean AGCM and nested model precipitation is shown in Figs. 5 b,c respectively. The superiority of the nested model precipitation simulation is immediately evident. The AGCM simulation grossly overestimates the summer precipitation over much of the continent. The nested model correctly simulates the precipitation maxima over the northwest and eastern coastal areas, as well as the gradient across the central U.S. and the minima over the western U.S.

(Fig. 5c). The main weakness in the nested model simulation is the less than observed precipitation over the far southeast U.S., the gulf of Mexico and the Atlantic. Poor simulation of the North American summer precipitation is a common problem in many AGCMs. Similar deficiencies were found in an examination of the North American summer precipitation simulated by the NCEP T62 and NCAR CCM3 AGCMs (not shown).

The simulated ensemble mean upper level wind, height and temperature fields have also been compared to observations, and in general, the AGCM and nested model error fields are quite similar (not shown). For example, relative to NCEP reanalyses, the AGCM 300 hPa geopotential height field has negative biases in the range of 60-90 m, whereas the nested model has broader negative biases in the range of 30-60 m.

b. Winter

The five-year mean January-February-March (JFM) 2 meter temperature obtained from the Ropelewski et al. (1985) station data is shown in Fig 6a. The corresponding ensemble mean height-corrected errors for the AGCM and the nested model are shown in Figs. 6 b,c respectively. Both models have significant positive errors of 4°C or more over the northern continent, but the AGCM errors are larger and extend southward into the central U.S. The nested model negative bias over the eastern U.S. reaches 4°C or more; whereas, the AGCM negative bias in the same region is roughly half that magnitude. In general, the North American continental winter season surface temperature simulations of the two models though somewhat different, have large errors.

The observed five-year mean JFM precipitation (Xie and Arkin, 1996) is shown in Fig. 7a. The corresponding ensemble mean AGCM and nested model precipitation is shown

in Figs. 7 b,c respectively. The AGCM simulation overestimates the precipitation over much of the continent, though not as badly as it did in summer. The nested model correctly simulates the precipitation maximum over the northwest coast and the minimum in the central continent. However, the northwest coast maximum is somewhat overestimated and the southeast U.S. and the Gulf of Mexico maximum is underestimated. The AGCM also has a low bias over the southeast U.S. Overall, the winter precipitation simulation of the nested model is superior to that of the AGCM alone, but the differences between the AGCM and the nested model are not as large as they were in summer. The JFM ensemble mean errors in the upper level wind, height and temperature fields are very similar between the AGCM and nested model (not shown), and are larger in magnitude than those during summer.

4. Interannual variability

In order to be useful for practical climate applications, a nested model must be able to simulate features of the observed interannual variability that are due to either local boundary forcing, such as soil wetness or snow effects, or remote boundary forcing, such as SST effects that are felt by the nested model through the lateral boundaries. The simulated AGCM and nested model interannual variability was compared to the observed interannual variability. In general, the nested model simulations of the interannual variability are similar and perhaps somewhat improved compared to that simulated by the AGCM alone. For the sake of brevity, only one summer and one winter case are presented in detail, chosen because of the large climate anomalies observed. The skill of the two models in general is compared by analyzing area-averaged systematic errors and root mean square errors for each year.

a. Summer

During April, May and June of 1988 low rainfall caused a severe drought in the corn belt of the central U.S. that left the region dry for the remainder of the summer. During June and July of 1993, persistent heavy rainfall caused severe flooding all along the Mississippi river basin. Although each of these two unconnected events had unique characteristics and life cycles, the difference between them is striking and presents a strong and important climatic signal that must be simulated by models that are to be used for climate prediction. A brief summary of how the AGCM and nested models simulated this signal is presented here.

The 1993 versus 1988 lower boundary forcing differences for the AGCM and the nested model were nearly identical. The models had identical SST forcing (Reynolds and Smith, 1994), and similar positive 1993 minus 1988 initial soil wetness differences in the corn belt of the U.S. (not shown).

The observed June-July mean 2-meter temperature difference for 1993 minus 1988 obtained from station data (Ropelewski et al., 1985) is shown in Fig 8a. The corresponding three-member ensemble mean temperature differences for the AGCM and the nested model are shown in Figs. 8 b,c respectively. Both models simulate a large region of relatively colder temperature for 1993 in the central U.S., though both center the region somewhat east of that observed, and neither produces the observed magnitude (6-8 °C). Although the two model simulations are largely similar, the nested model better simulates the magnitude of the observed anomaly, reaching 4 °C. The AGCM also extends the anomaly more southward

than observed.

The observed June-July mean 1993 minus 1988 precipitation difference (Xie and Arkin, 1996) is shown in Fig. 9a. The corresponding three-member ensemble mean precipitation differences for the AGCM and the nested model are shown in Figs. 9 b,c, respectively. Prominent in the observations is a broad 1 mm day^{-1} positive precipitation difference that spans much of the central U.S. and reaches over 4 mm day^{-1} over the upper Mississippi basin. The AGCM does not simulate this signal at all, but rather has weaker positive differences both eastward and southward of the observed positive difference. The nested model does a far better job of simulating the broad 1 mm day^{-1} difference, though it extends it a bit too far southward and eastward. The nested model also properly places the center of the large difference over the corn belt with a maxima of over 3 mm day^{-1} , which is somewhat less than that observed. The surprising difference in the ability of the two models to simulate this large and important signal merits further analysis.

The precipitation differences in this region can be accounted for by summing the precipitable water, evaporation and vertically integrated moisture flux convergence differences in the region. The precipitation and evaporation differences in each model were internally consistent with each other; however, it is only in the nested model that the location of the precipitation and evaporation anomalies were correctly simulated. The major component of the precipitation differences in both models was the vertically integrated moisture flux convergence differences which reached 2-3 mm day^{-1} in magnitude and were coincident with the simulated precipitation differences in each model (not shown). An examination of the June-July mean NCEP reanalysis 850 hPa meridional wind difference

showed that the observed positive moisture convergence difference in upper Mississippi basin was due to an enhanced southerly jet south of 40°N and relative northerly flow to the north (not shown). The ensemble mean June-July simulated 850 hPa meridional wind differences for the AGCM and the nested model both contain similar features, but the AGCM places the convergence too far south compared to that observed (not shown). Thus the difference in the two models' simulation of the observed 1993-1988 precipitation differences is related to their ability to simulate both the local evaporation and meridional flow differences.

b. Winter

The winter years chosen in this study include 1982-1983, which had large positive SST anomalies in the tropical Pacific accompanied by strong climate anomalies over North America, and 1988-89, which had large negative SST anomalies in the tropical Pacific. The winter of 1982-83 was warm over most of the U.S., cold over much of Canada and was wet along the west and southeast coasts. The winter of 1988-89 had much weaker anomalies over North America, thus differences between the two years reflect mainly the strong 1982-83 anomalies.

The observed JFM 1989 minus JFM 1983 2-meter surface temperature differences calculated from the Ropelewski et al., (1985) station data, contain a broad region of large negative differences across the northern U.S./ southern Canada and a band of positive differences to the north (Fig. 10a). The AGCM (Fig. 10b) and the nested model (Fig. 10c) ensembles simulate negative differences across the entire northeast half of the continent that are quite similar to each other, but quite different from the observed anomalies.

differences simulated by the nested model contain more details than those simulated by the AGCM alone, particularly in regions with strong orographic features. However, one feature simulated by the AGCM but missed by the nested model is the positive difference that extends from south of the Great Lakes to Oklahoma in the observations.

c. Systematic error and root mean square error

To facilitate objective evaluation of the relative skills of the AGCM and the nested model, the seasonal mean systematic errors and root mean square (RMS) errors for 2-meter temperature and precipitation have been calculated and area-averaged over the entire land surface area included in Figs. 4 through 11. The systematic errors are given in Table 2, the RMS errors are given in Table 3.

TABLE 2. Systematic error averaged over 162°W - 60°W, 20°N - 70°N, land only. Years for summer are: 1986,'87,'88,'93,'94. Years for winter are: 1983,'85,'87,'89,'91.

	Surface Temperature (°C)				Precipitation (mm day^{-1})			
	Summer (JJAS)		Winter (JFM)		Summer (JJAS)		Winter (JFM)	
	COLA AGCM	COLA + Eta	COLA AGCM	COLA + Eta	COLA AGCM	COLA + Eta	COLA AGCM	COLA + Eta
Year 1	1.72	-0.84	3.23	0.35	0.95	-0.24	0.70	-0.04
Year 2	0.75	-1.65	2.40	-0.29	1.11	-0.13	0.59	-0.14
Year 3	0.91	-1.20	1.96	-1.63	1.13	-0.34	0.81	0.04
Year 4	0.67	-1.92	2.08	-1.06	1.03	-0.18	0.90	0.03
Year 5	0.83	-1.56	1.10	-1.35	1.22	-0.06	0.94	0.12
Mean	0.98	-1.43	2.15	-0.79	1.09	-0.19	0.79	0.00

Both models exhibit large systematic temperature biases in both seasons. The AGCM is too warm relative to the observations in all 10 cases, and the nested model is too cold compared to observations in nine out of 10 cases. The AGCM temperature biases are larger in winter than in summer. The nested model biases are similar in magnitude in the two seasons. The nested model biases are larger (smaller) in magnitude than those of the AGCM alone in summer (winter).

Positive systematic precipitation biases of roughly 1 mm day^{-1} occur in the AGCM simulations in all cases. The nested model has much smaller systematic precipitation biases, that are negative in most of the cases, but never exceed 0.34 mm day^{-1} in magnitude.

TABLE 3. Root mean square error averaged over 162°W - 60°W, 20°N - 70°N, land only. Years for summer are: 1986,'87,'88,'93,'94. Years for winter are: 1983,'85,'87,'89,'91.

	Surface Temperature (°C)				Precipitation (mm day^{-1})			
	Summer (JJAS)		Winter (JFM)		Summer (JJAS)		Winter (JFM)	
	COLA AGCM	COLA + Eta	COLA AGCM	COLA + Eta	COLA AGCM	COLA + Eta	COLA AGCM	COLA + Eta
Year 1	2.83	1.58	5.86	4.87	1.86	0.95	1.71	0.99
Year 2	2.25	2.24	4.68	4.29	1.87	0.93	1.41	1.05
Year 3	2.20	1.99	4.58	4.39	1.93	1.07	1.53	0.90
Year 4	1.95	2.35	4.89	4.11	1.97	1.16	1.51	1.20
Year 5	1.95	2.18	3.92	5.03	2.10	0.97	1.62	1.02
Mean	2.24	2.07	4.79	4.54	1.95	1.02	1.56	1.03

Due to the large systematic biases noted above, the area-average RMS error in temperature is relatively large in both seasons and in both models. It is much larger in the winter season in both models (about 5°C), than in the summer season (about 2°C). This is likely due to the much larger temperature gradients and variability during the winter season, but may also be due in part to the positive impact of land surface processes on the summer temperature simulations. Overall, there is little difference in the RMS error in temperature between the two models.

The AGCM precipitation RMS error is between 1.9 and 2.1 mm day^{-1} in summer and between 1.4 and 1.7 mm day^{-1} in winter. The nested model precipitation RMS error is between 0.9 and 1.2 mm day^{-1} in both seasons, which is considerably less than that of the

AGCM alone. The calculations presented in Tables 2 and 3 confirm the impressions gained from examination of Figs. 4 through 7, that the 2-meter temperature simulations of both the models are poor, and the precipitation simulations of the nested model are significantly better than those of the AGCM alone.

5. Signal to noise calculations

From an analysis of the interannual anomalies simulated by both models (including those discussed in the previous section) it appears that the nested model is capable of simulating most of the interannual anomalies simulated by the AGCM alone and, in some cases, is capable of enhancing them or even simulating anomalies missed by the AGCM. From a wealth of climate studies with AGCMs, it is well known that ensembles of simulations are required in order to obtain some measure of the significance and reliability of climate simulations. An important question is whether the ensemble size required for nested models is similar or different from that required for AGCMs alone. Although the ensemble sizes used in this preliminary study are modest, an attempt is made to shed light on this question by analyzing the interannual climate signal, the intra-ensemble noise and the signal-to-noise ratios of the nested model simulations in comparison to those in the AGCM simulations. Despite the small ensemble size, the comparison between the AGCM and nested model results is useful because the calculation is done in an identical fashion for both.

The signal to noise ratio σ_S^2 / σ_N^2, is defined as the ratio between the interannual climate signal given by

$$\sigma_S^2 = \sum_{j=1}^{m} \left(E_j - C\right)^2 / (m-1) \qquad (1)$$

and the intra-ensemble noise given by

$$\sigma_N^2 = \sum_{j=1}^{m} \frac{\left[\sum_{i=1}^{n} \left(r_{ij} - E_j\right)^2 / (n-1)\right]}{m} \qquad (2)$$

where i is an individual member (of the n=3 size ensemble) for a given year j (of m=5 total years), E_j is the model ensemble mean for a given year j, given by

$$E_j = \sum_{i=1}^{n} r_{ij} / n \qquad (3)$$

and r_{ij} is integration i of the ensemble for year j. The five-year mean ensemble C, is given by

$$C = \sum_{j=1}^{m} E_j / m \qquad (4)$$

An examination of σ_S^2 , σ_N^2 and σ_S^2/σ_N^2 for the AGCM and the nested model simulations for the 2-meter temperature and precipitation fields shows that the signal and noise fields appear quite similar for the AGCM and the nested model. Differences show up better in the signal-to-noise ratio. The JJAS (JFM) signal-to-noise ratios of the 2-meter temperature and precipitation are shown in Fig.12 (13) for land areas only. In each figure there are four frames: a) AGCM temperature, b) nested model temperature, c) AGCM precipitation and d) nested model precipitation.

In general, the signal-to-noise ratios between the AGCM and the nested model are similar for a given field and season. In both seasons, the signal-to-noise ratio is generally larger in magnitude and more spatially coherent for temperature than for precipitation. Also, in general, the summer (JJAS) signal-to-noise ratios of both temperature and precipitation have maxima in the central continent, and the winter (JFM) signal-to-noise ratio maxima are more widespread, with some tendency towards maxima in coastal areas. This is consistent with the role of land surface processes on atmospheric predictability, which is more prominent in the interior of continents and in the summer season (Karl, 1983). It is also consistent with the positive impact of SST anomalies on predictability, which is more prominent along the coasts and during the winter season (Ropelewski and Halpert, 1989, 1996).

The limited sample size inhibits analysis of the detailed differences between the AGCM and nested model fields. However, in the winter season, the nested model tends to have larger signal-to-noise ratios in both temperature and precipitation than does the AGCM alone. In summer, the two models are quite similar, though the AGCM temperature signal-

to-noise ratio is higher over the southeastern U.S. than that of the nested model. The most important point to note is the fact that the signal-to-noise ratios of the nested model are in general not less than those of the AGCM alone, despite the smaller scales resolved by the nested model.

6. Conclusions

An examination of 15 North American seasonal winter simulations and 15 North American seasonal summer simulations with the NCEP Eta model nested in the COLA AGCM shows that the nested model significantly improves upon the seasonal precipitation simulations of the AGCM alone, and retains the interannual variability present in the AGCM simulations. The simulation of both the finer scale details and the overall seasonal mean precipitation pattern were improved in the nested model. An examination of several other simulated atmospheric variables showed that the nested model simulations were generally as good or better than those of the AGCM. The interannual variability was not only conveyed from the AGCM to the nested model, but was improved in some cases. It is not apparent whether the cause for this improvement was the different physics, the enhanced resolution or the better representation of orography in the nested model, or some combination of the three. In particular, the precipitation difference between the 1988 U.S. drought and 1993 U.S. flood was much better simulated by the nested model.

In addition to getting a reasonable simulation of the seasonal mean precipitation, it is important for regional applications that a model correctly simulate the intraseasonal variability, particularly for precipitation. In a companion study, Shukla et al. (1998) have examined the AGCM and nested model simulations of the daily precipitation variability over

different regions of the U.S. and found that the nested model produced a more realistic simulation of intraseasonal variability compared to the AGCM alone. Those results, in combination with the results presented here, make it clear that the nested model captures both the mean precipitation and the precipitation variability better than the AGCM alone.

Despite the relatively small sample size, an attempt was made to make an estimate of the signal to noise characteristics of the nested simulations compared to that of the AGCM simulations. The signal, noise and signal-to-noise-ratios of the near surface temperature and precipitation fields were generally similar between the nested model and AGCM simulations. However, in the winter season the nested model tends to have larger signal-to-noise ratios in both temperature and precipitation compared to the AGCM. This result was somewhat unexpected because classical studies on the scale dependance of predictability suggest that a higher resolution model should allow errors in smaller scale features to grow faster and generate a higher level of noise. If these results are valid for other cases, it could be concluded that the ensemble size required for nested climate integrations may not be larger than that required for AGCM integrations.

This study should be viewed in the context of the larger problem of regional climate prediction and assessment (Fig. 1). These results are encouraging as they show that it is possible to go from AGCM seasonal forecasts of planetary waves to regional forecasts of precipitation with a reasonable ensemble size. To quantify the requirements for ensemble size, more tests involving larger ensembles and different seasons and years are required. Then it might even be possible to go on to the next step of driving even smaller scale models of hydrology and water management, using output from the nested regional model.

Acknowledgements

Acknowledgments. The authors would like to thank Y. Ji and E. Altshuler for help with technical aspects of the model simulations and T. Black, K. Mitchell, F. Mesinger and Z. Janjic for useful discussions on aspects of the Eta model. All the Eta model calculations were done on NASA Center for Computational Sciences computers at Goddard Space Flight Center. This research was supported by NOAA grant NA-76-GP0258, NASA grants NAGW-5213, and by NSF grant ATM-93-21354.

References

Alpert, J. C., M. Kanamitsu, P. M. Caplan, J. G. Sela, G. H. White and E. Kalnay, 1988: Mountain induced gravity wave drag parameterization in the NMC medium-range forecast model. Proceedings of the Eight AMS Conference on Numerical Weather Prediction, 22-26 February, 1988, AMS, Boston, MA, 726-733.

Arakawa, A., and V. R. Lamb, 1977: Computational design of the basic dynamical processes of the UCLA general circulation model. *Methods Comput. Phys.*, **17,** 173-265.

Arakawa, A., and W. H. Schubert, 1974: Interaction of cumulus cloud ensemble with the large-scale environment. *J. Atmos. Sci.*, **31,** 671-701.

Betts, A. K., and M. T. Miller, 1986: A new convective adjustment scheme. Part II: Single column tests using GATE wave, BOMEX, and Arctic air-mass data. *Quart. Roy. Meteor. Soc.*, **112,** 693-703.

Black, T., 1994: The new NMC mesoscale Eta model: description and forecast examples. *Wea. Forecasting,* **9,** 265-278.

Chen, F., Z. Janjic and K. Mitchell, 1997: Impact of atmospheric surface layer parameterization in the new land-surface scheme of the NCEP mesoscale ETA numerical model. *Bound.-Layer Meteor.*, **85,** 391-421.

DeWitt, D.G., 1996: The effect of cumulus convection on the climate of COLA general circulation model. *COLA Technical Report #27.* Available from Center for Ocean-Land-Atmosphere Studies, 4041 Powder Mill Road, Suite 302, Calverton, MD 20705.

Dorman, J.L. and P. Sellers, 1989: A global climatology of albedo, roughness length and stomatal resistance for atmospheric general circulation models as represented by the Simple Biosphere Model (SiB). *J. Appl. Meteor.*, **28,** 833-855.

Fels, S. B., and M. D. Schwarzkopf, 1975: The simplified exchange approximation: A new method for radiative transfer calculations. *J. Atmos. Sci.*, **32,** 1475-1488.

Fennessy, M. J. and J. Shukla, 1996: Impact of initial soil wetness on seasonal atmospheric prediction. *COLA Technical Report #34.* Available from Center for Ocean-Land-Atmosphere Studies, 4041 Powder Mill Road, Suite 302, Calverton, MD 20705.

Fennessy, M. J. and Y. Xue, 1997: Impact of USGS vegetation map on GCM simulations over the United States. *Ecological Applications, 7,* 22-23.

Giorgi, F., 1990: Simulation of regional climate using a limited area model nested in a general circulation model. *J. Climate,* **3,** 941-963.

Giorgi, F. and G. T. Bates, 1989: The climatological skill of a regional model over complex terrain. *Mon. Wea. Rev.,* **117,** 2325-2347.

Harshvardhan, R. Davies, D. A. Randall and T. G. Corsetti, 1987: A fast radiation parameterization for general circulation models. *J. Geophys. Res.,* **92,** 1009-1016.

Hogan, T. F., and T. E. Rosmond, 1991: The description of the Navy operational global atmospheric prediction system's spectral forecast model. *Mon. Wea. Rev.,* **119,** 1786-1815.

Hou, Y.-T., 1990: Cloud-Radiation-Dynamics Interaction. Ph.D. Thesis, Dept. of Meteorology, University of Maryland, College Park, MD 20742.

Janjic, Z. I., 1984: Nonlinear advection schemes and energy cascade on semi-staggered grids.. *Mon. Wea. Rev.,* **112,** 1234-1245.

Janjic, Z. I., 1990: The step-mountain coordinate: physical package. *Mon. Wea. Rev.,* **118,** 1429-1443.

Janjic, Z. I., 1994: The step-mountain Eta coordinate model: further developments of convection, viscous sublayer, and turbulence closure schemes. *Mon. Wea. Rev.,* **122,** 927-945.

Ji, Y., 1996: Modeling the Asian summer monsoon with high resolution regional Eta model: The impact of sea surface temperature anomaly associated with ENSO cycle. Ph.D. dissertation. University of Maryland at College Park, 139 pp. [Available from University Microfilm, The University of Maryland at College Park, College Park, MD 20742.]

Ji, Y., and A. D. Vernekar, 1997: Simulation of the Asian summer monsoons of 1987 and 1988 with a regional model nested in a global GCM. *J. Climate,* **10,** 1965-1979.

Karl, T. R., 1983: Some spatial characteristics of drought duration in the United States. *Climate Appl. Meteor.,* **22,** 1356-1366.

Kinter III, J. L., J. Shukla, L. Marx and E. K. Schneider, 1988: A simulation of the winter and summer circulations with the NMC global spectral model. *J. Atmos. Sci.,* **45,** 2486-2522.

Kinter, J. L. III, D. DeWitt, P. A. Dirmeyer, M. J. Fennessy, B. P. Kirtman, L. Marx, E. K. Schneider, J. Shukla and D. M. Straus, 1997: The COLA atmosphere-biosphere

general circulation model. Volume 1: Formulation. *COLA Technical Report #51.* Available from Center for Ocean-Land-Atmosphere Studies, 4041 Powder Mill Road, Suite 302, Calverton, MD 20705.

Lacis, A. A. and J. E. Hansen, 1974: A parameterization for the absorption of solar radiation in the Earth's atmosphere. *J. Atmos. Sci.*, **31**, 118-133.

Lobocki, L., 1993: A procedure for the derivation of surface-layer bulk relationships from simplified second-order closure models. *J. Appl Meteor.*, **32**, 126-138.

Mellor, G. L. and T. Yamada, 1982: Development of a turbulence closure model for geophysical fluid problems. *Rev. Geophys. Space Phys.*, **20,** 851-875.

Mesinger, F., 1984: A blocking technique for representation of mountains in atmospheric models. *Riv. Meteor. Aeronaut.*, **44,** 195-202.

Mesinger, F., 1995: The eta regional model and its performance at the U.S. National Centers for Environmental Prediction. *Int. Workshop on Limited-Area and Variable Resolution Models, Beijing China,* World Meteorological Organization, 19-28.

Mesinger, F., 1996: Improvements in quantitative precipitation forecasts with the Eta regional model at the National Centers for Environmental Prediction: The 48-km upgrade. *Bull. Amer. Meteor. Soc.*, **77,** 2637-2649.

Mesinger, F., and T. L. Black, 1992: On the impact of forecast accuracy of the step-mountain (eta) vs. sigma coordinate. *Meteor. Atmos. Phys.*, **50,** 47-60.

Mesinger, F., Z. I. Janjic, S. Nickovic, D. Gavrilov and D. G. Deaven, 1988: The step-mountain coordinate: model description and performance for cases of Alpine lee cyclogenesis and for a case of an Appalachian redevelopment. *Mon. Wea. Rev.*, **116,** 1493-1518.

Miyakoda, K. and J. Sirutis, 1977: Comparative integrations of global spectral models with various parameterized processes of subgrid scale vertical transports. *Beitr. Phys. Atmos.*, **50,** 445-447.

Moorthi, S., and M. J. Suarez, 1992: Relaxed Arakawa-Schubert: A parameterization of moist convection for general circulation models. *Mon. Wea. Rev.*, **120,** 978-1002.

Philips, N. A., 1957: A coordinate system having some special advantages for numerical forecasting. *J. Meteor.*, **14,** 184-185.

Posey, J. W. and P. F. Clapp, 1954: Global distribution of normal surface albedo. *Geofisica Int.*, **4,** 33-48.

Reynolds, R. W. and T. M. Smith, 1994: Improved global sea surface temperature analyses using optimum interpolation. *J. Climate,* **7,** 929-948.

Rogers, E., T. L. Black, D. G. Deaven, G. J. DiMego, Q. Zhao, M. Baldwin, N. W. Junker and Y. Lin, 1996: Changes to the operational "early" Eta analysis/forecast system at the National Centers for Environmental Prediction. *Wea. Forecasting,* **11,** 391-413.

Rogers, E., D. G. Deaven, G. J. DiMego, 1995: The regional analysis system for the operational "early" Eta model: original 80-km configuration and recent changes. *Wea. Forecasting,* **10**, 810-825.

Ropelewski, C. F., and M. F. Halpert, 1989: Precipitation patterns associated with the high index phase of the Southern Oscillation. *J. Climate,* **2,** 268-284.

Ropelewski, C. F., and M. F. Halpert, 1996: Quantifying Southern Oscillation precipitation regimes. *J. Climate,* **9,** 1043-1059.

Ropelewski, C. F., J. E. Janowiak and M. F. Halpert, 1985: The analysis and display of real time surface climate data. *Mon. Wea. Rev.,* **113,** 1101-1107.

Sato, N., P. J. Sellers, D. A. Randall, E. K. Schneider, J. Shukla, J. L. Kinter III, Y-T. Hou and E. Albertazzi, 1989: Effects of implementing the Simple Biosphere Model in a general circulation model. *J. Atmos. Sci.,* **46,** 2757-2782.

Sela, J. G., 1980: Spectral modeling at the National Meteorological Center. *Mon. Wea. Rev.*, **108**, 1279-1292.

Sellers, P. J., Y. Mintz, Y. C. Sud and A. Dalcher, 1986: A simple biosphere model (SiB) for use within general circulation models. *J. Atmos. Sci.* **43**, 505-531.

Shukla, J., 1998: Predictability in the midst of chaos: A scientific basis for climate forecasting, *Science*, **282**, pp. 728-731.

Shukla, J., M. Fennessy, J. Kinter, B. Kirtman, L. Marx, D. Paolino, D. DeWitt, P. Dirmeyer, B. Doty, B. Huang, E. Schneider, D. Straus, Z. Zhu, 1998: Six-month lead prediction of regional climate using dynamical models: A case study of winter (JFM) 1998 in North America. Submitted to *Bull. Amer. Meteor. Soc.*

Slingo, J. M., 1987: The development and verification of a cloud prediction scheme for the ECMWF model. *Quart. J. Roy. Meteor. Soc.,* **103,** 29-43.

Tanajura, C., 1996: Modeling and Analysis of the South American Summer Climate. Ph.D. Dissertation, University of Maryland.

Tiedtke, M., 1984: The effect of penetrative cumulus convection on the large-scale flow in a general circulation model. *Beitr. Phys. Atmos.*, **57**, 216-239.

Vernekar, A. , B. Kirtman, J. Zhou and D. DeWitt, 1992: Orographic gravity-wave drag effects on medium-range forecasts with a general circulation model. *Physical Processes in Atmospheric Models*, Editors: D. R. Sikka and S. S. Singh, Wiley Eastern Limited, New Delhi, 295-307.

Xie, P. and P. Arkin, 1996: Analysis of global monthly precipitation using gauge observations, satellite estimates, and numerical model predictions. *J. Climate,* **9,** 840-858.

Xue, Y., P. J. Sellers, J. L. Kinter and J. Shukla, 1991: A simplified biosphere model for global climate studies. *J. Climate,* **4,** 345-364.

Zhao, Q., T. L. Black and M. E. Baldwin, 1997: Implementation of the cloud prediction scheme in the Eta model at NCEP. *Wea. Forecasting,* **12,** 697-711.

Figures

Fig.1. Scientific basis for regional assessment.

Fig. 2. Integration domain of the 80 km Eta used in this study (dark) and the March, 1997 operational 48 km Eta (light).

Fig. 3. Orography used for a) COLA AGCM, b) nested Eta and c) difference. Contours are 100, 200, 400, 800, 1200, 1600, 2000, 2400 m.

Fig. 4. JJAS 5-year ensemble mean 2-meter temperature for a) observations (see text), b) COLA AGCM error and c) nested Eta model error. Contour interval is 2°C in a, contours are ± 1, 2, 4, 6, 8 °C in b, c.

Fig. 5. JJAS 5-year ensemble mean precipitation for a) Xie/Arkin observations, b) COLA AGCM and c) nested Eta model. Contours are 1, 2, 3, 4, 6, 8 mm day^{-1}.

Fig. 6. JFM 5-year ensemble mean 2-meter temperature for a) observations (see text), b) COLA AGCM error and c) nested Eta model error. Contour interval is 4°C in (a), contours are ± 1, 2, 4, 6, 8 °C in (b), (c).

Fig. 7. JFM 5-year ensemble mean precipitation for a) Xie/Arkin observations, b) COLA AGCM and c) nested Eta model. Contours are 1, 2, 3, 4, 6, 8 mm day^{-1}.

Fig. 8. June-July mean 1993 minus 1988 2-meter temperature difference for a) observations (see text), b) COLA AGCM ensemble and c) nested Eta model ensemble. Contours are ± 1, 2, 4, 6, 8 °C.

Fig.9. June-July mean 1993 minus 1988 precipitation difference for a) Xie/Arkin observations, b) COLA AGCM ensemble and c) nested Eta model ensemble. Contours are ± 1, 2, 3, 4 mm day^{-1}.

Fig.10. JFM mean 1989 minus 1983 2-meter temperature difference for a) observations (see text), b) COLA AGCM ensemble and c) nested Eta model ensemble. Contours are ± 1, 2, 4, 6, 8 °C.

Fig.11. JFM mean 1989 minus 1983 precipitation difference for a) Xie/Arkin observations, b) COLA AGCM ensemble and c) nested Eta model ensemble. Contours are ± 1, 2, 3, 4 mm day^{-1}.

Fig.12. JFM signal-to-noise ratio (see text) for a) COLA AGCM 2-meter temperature, b) nested Eta model 2-meter temperature, c) COLA AGCM precipitation and d) nested Eta model precipitation.

Fig.13. JJAS signal-to-noise ratio (see text) for a) COLA AGCM 2-meter temperature, b) nested Eta model 2-meter temperature, c) COLA AGCM precipitation and d) nested Eta model precipitation.

Scientific Basis for Regional Assessment:

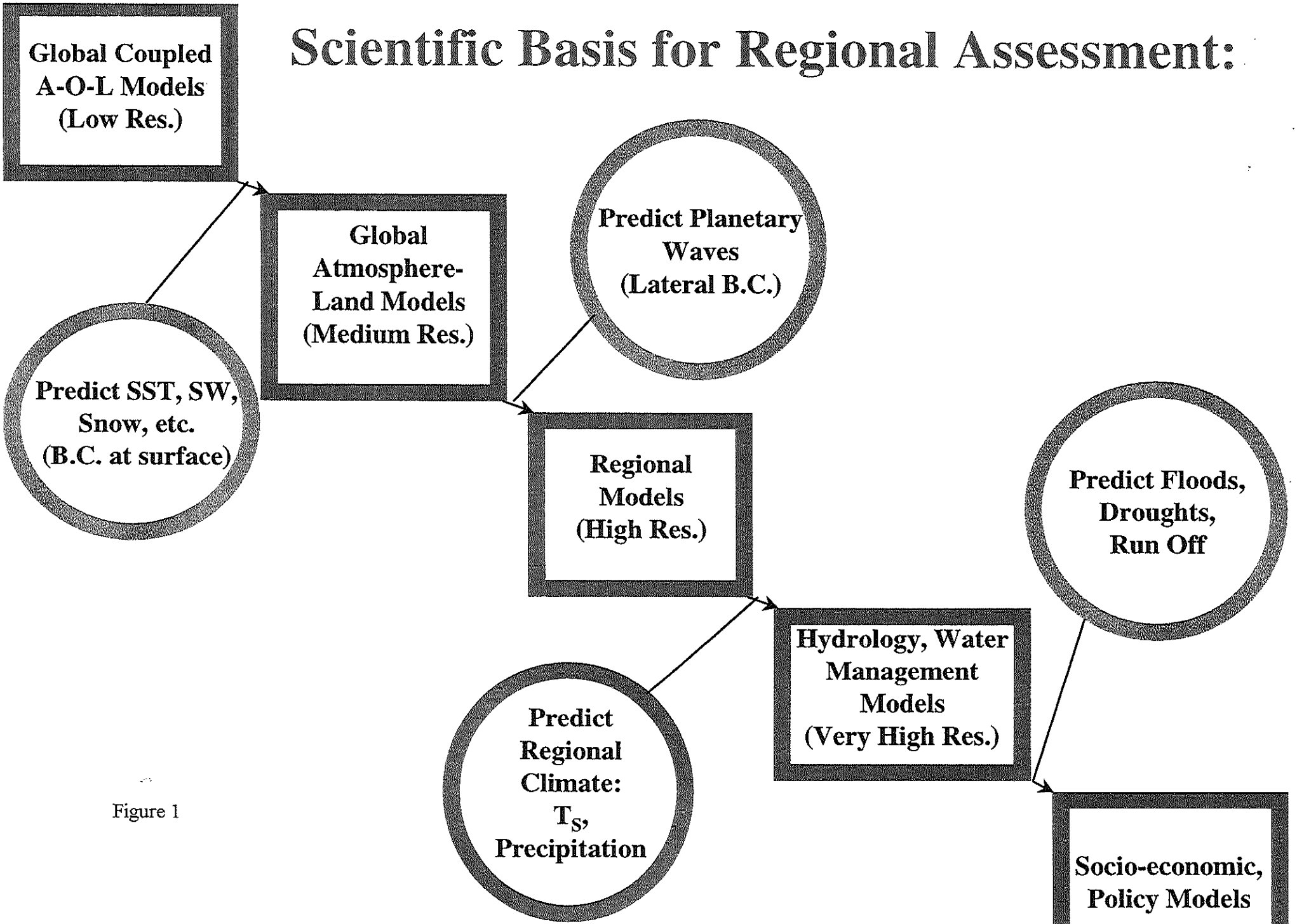

Figure 1

Center for Ocean-Land-Atmosphere Studies

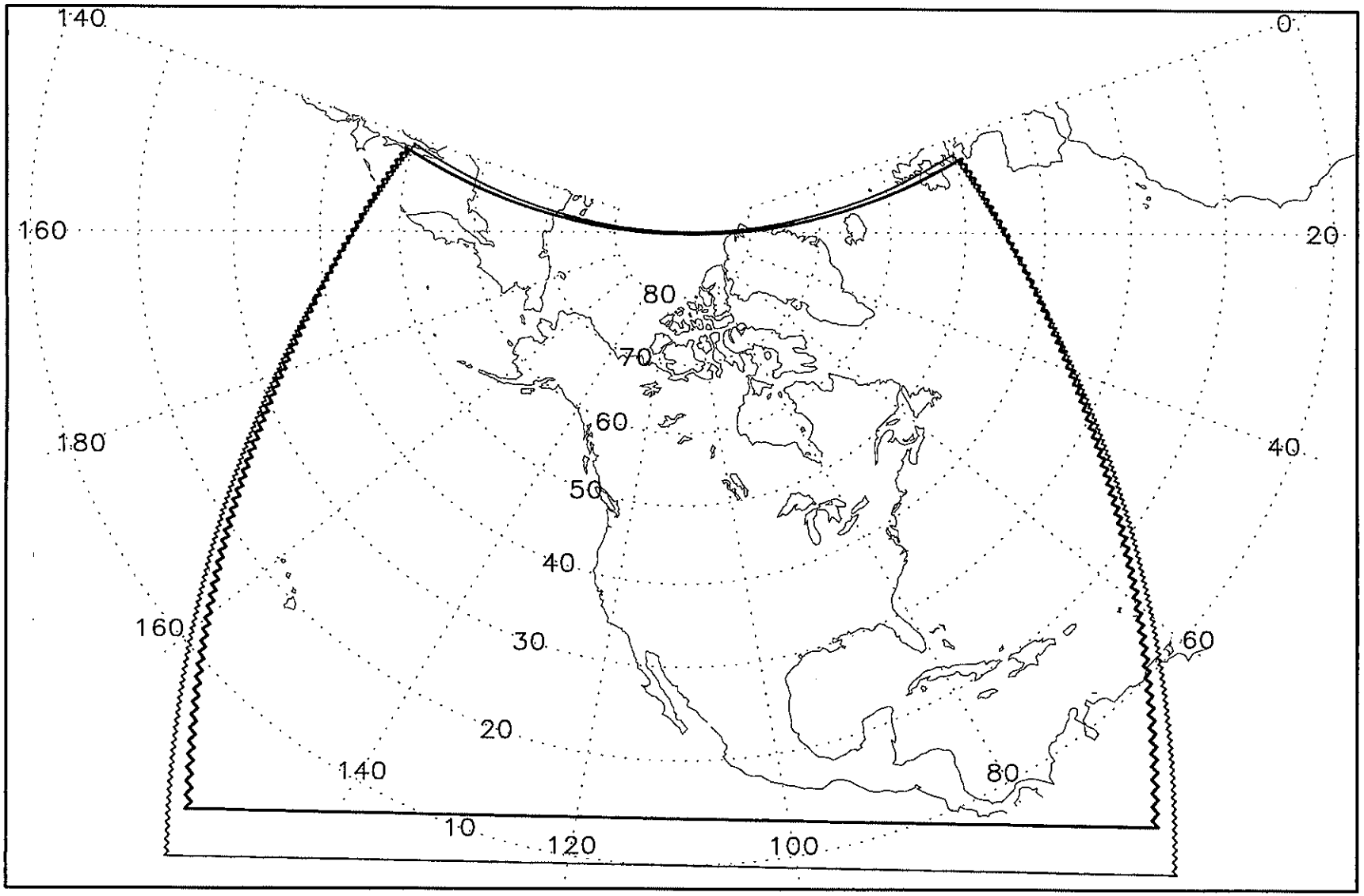

Figure 2

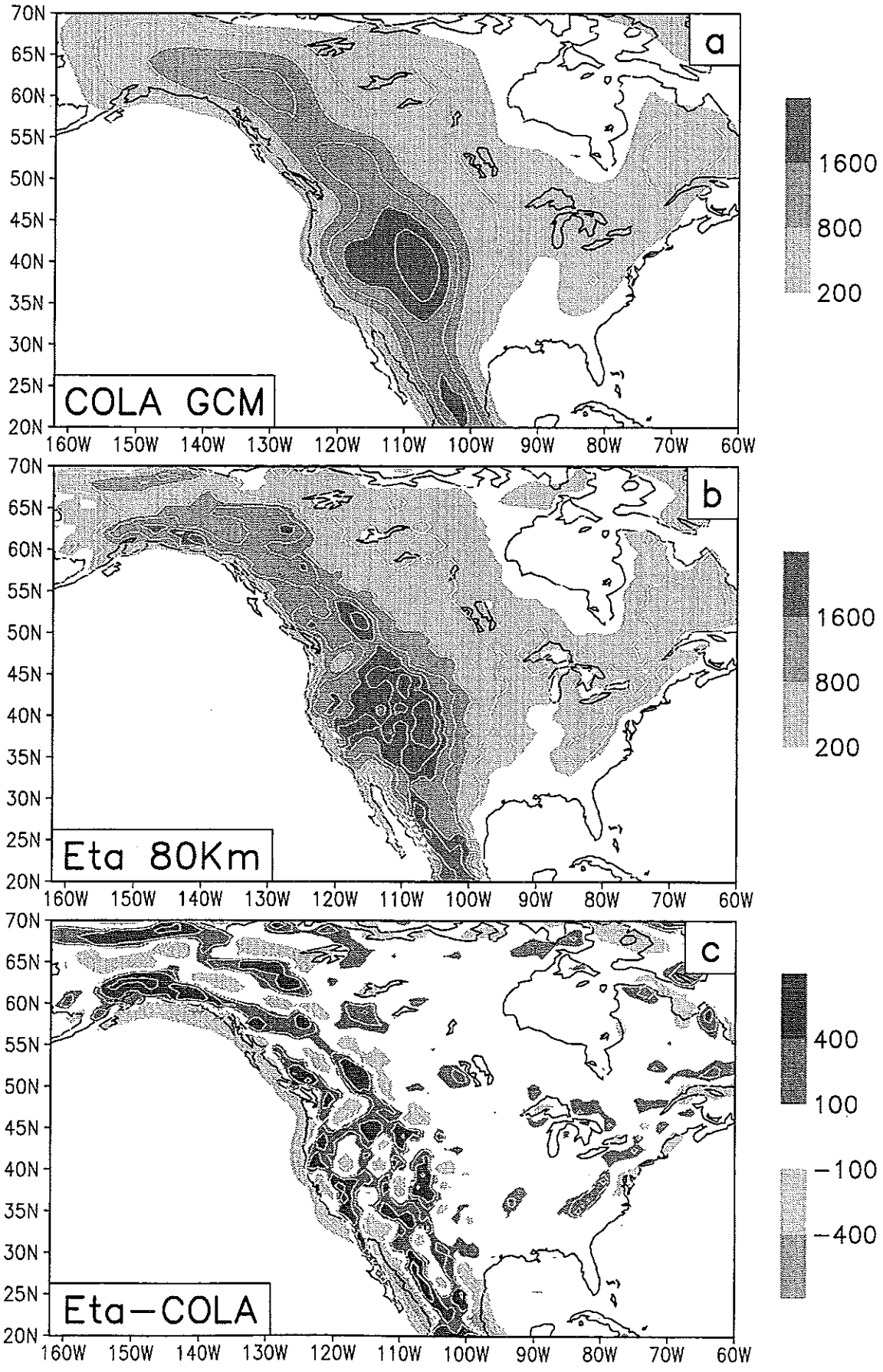
a
COLA GCM
1600
800
200
b
Eta 80Km
1600
800
200
c
Eta−COLA
400
100
−100
−400
70N
65N
60N
55N
50N
45N
40N
35N
30N
25N
20N
160W
150W
140W
130W
120W
110W
100W
90W
80W
70W
60W

Figure 3

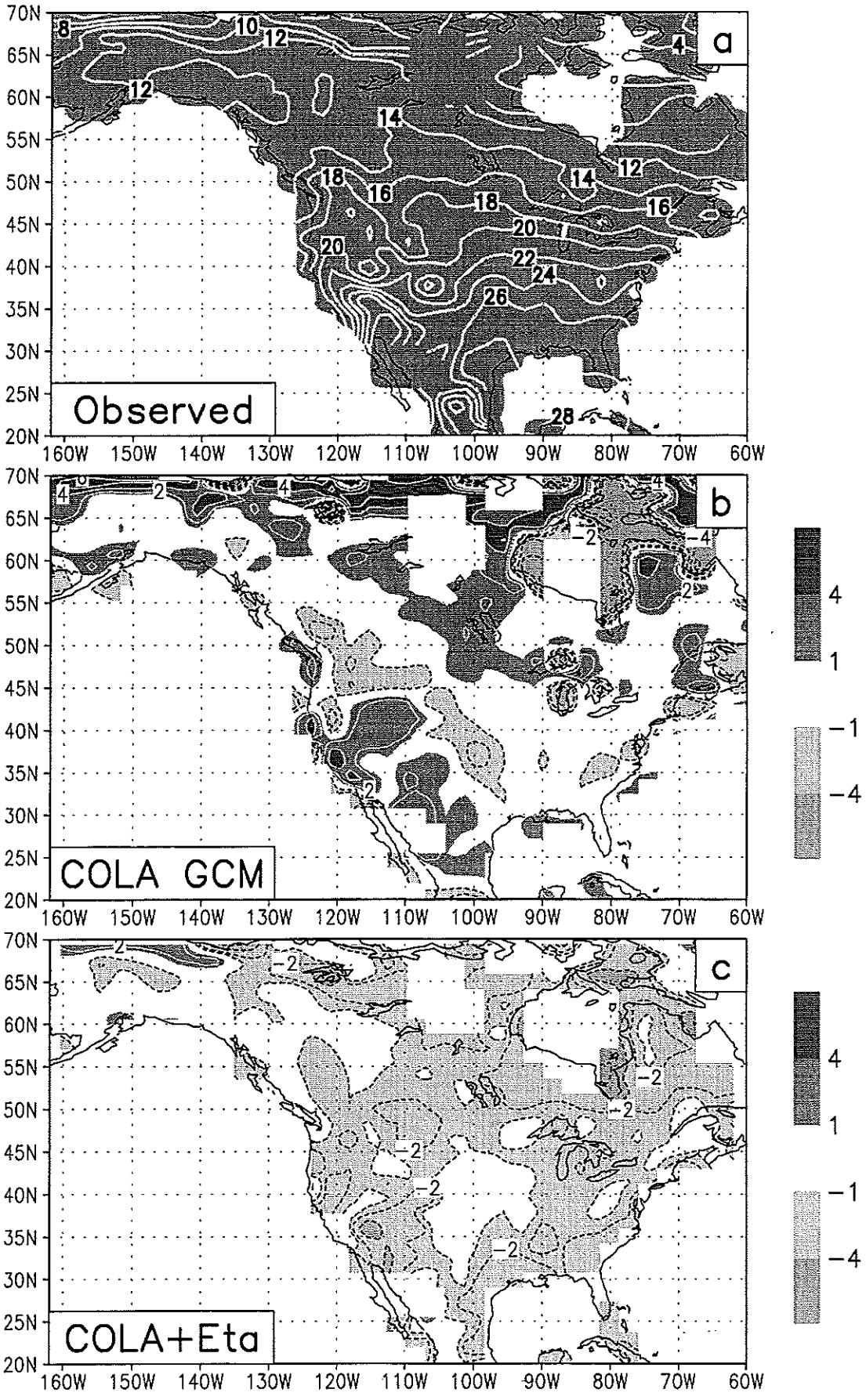
a
Observed
b
COLA GCM
c
COLA+Eta
70N
65N
60N
55N
50N
45N
40N
35N
30N
25N
20N
160W
150W
140W
130W
120W
110W
100W
90W
80W
70W
60W
4
1
−1
−4

Figure 4

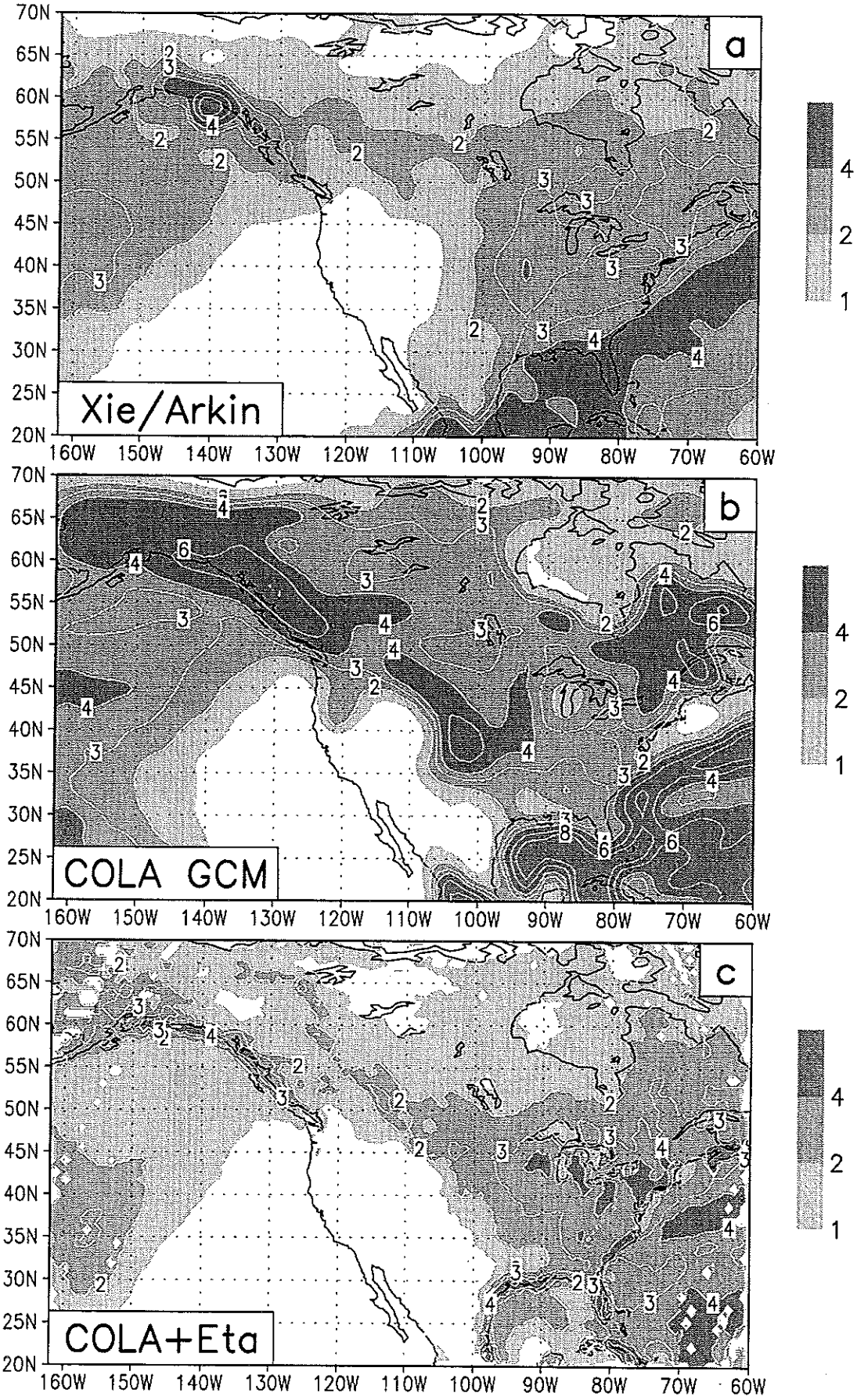
a
Xie/Arkin
b
COLA GCM
c
COLA+Eta
70N
65N
60N
55N
50N
45N
40N
35N
30N
25N
20N
160W
150W
140W
130W
120W
110W
100W
90W
80W
70W
60W
4
2
1

Figure 5

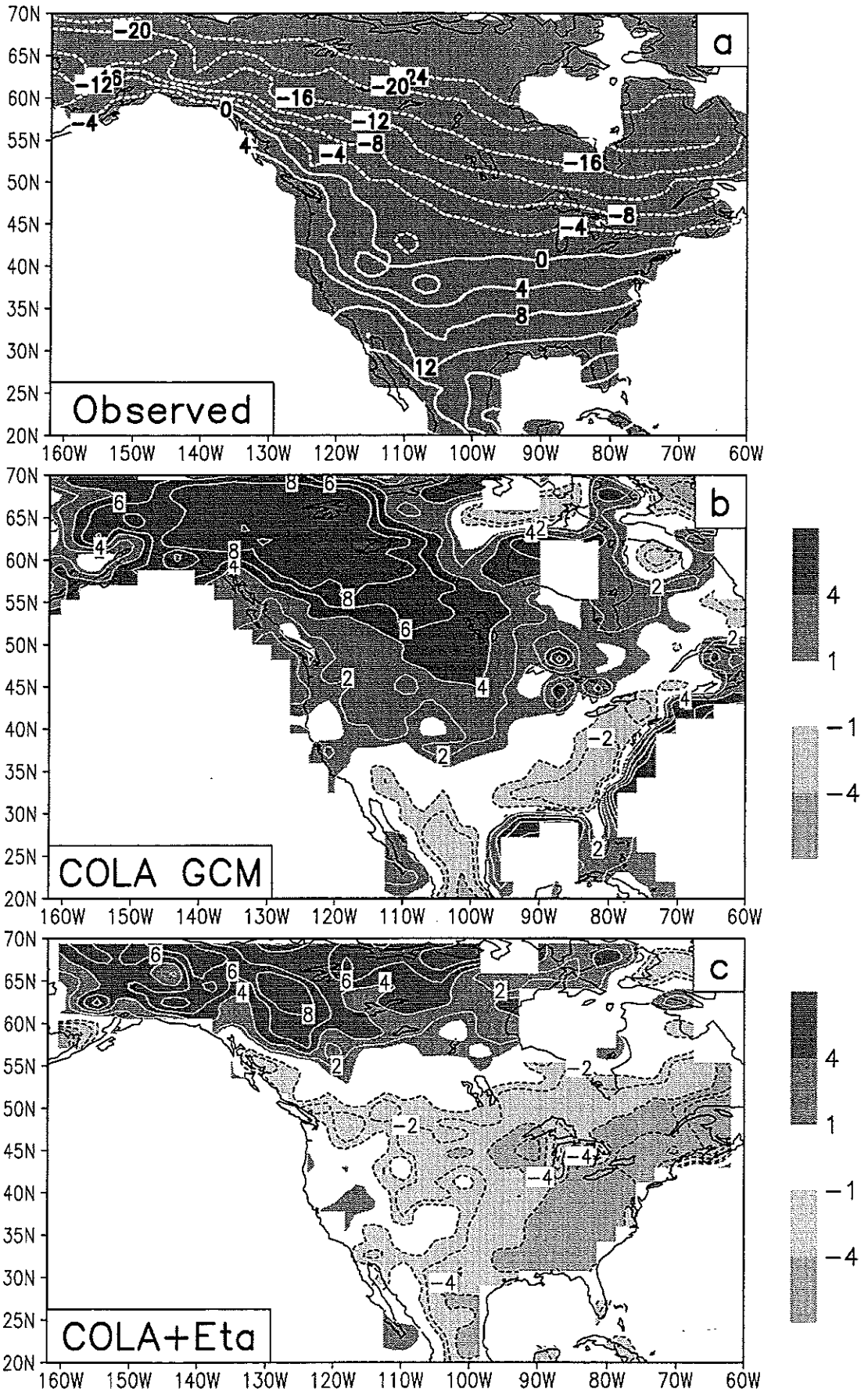
a
Observed
b
COLA GCM
c
COLA+Eta
70N
65N
60N
55N
50N
45N
40N
35N
30N
25N
20N
160W
150W
140W
130W
120W
110W
100W
90W
80W
70W
60W
4
1
−1
−4

Figure 6

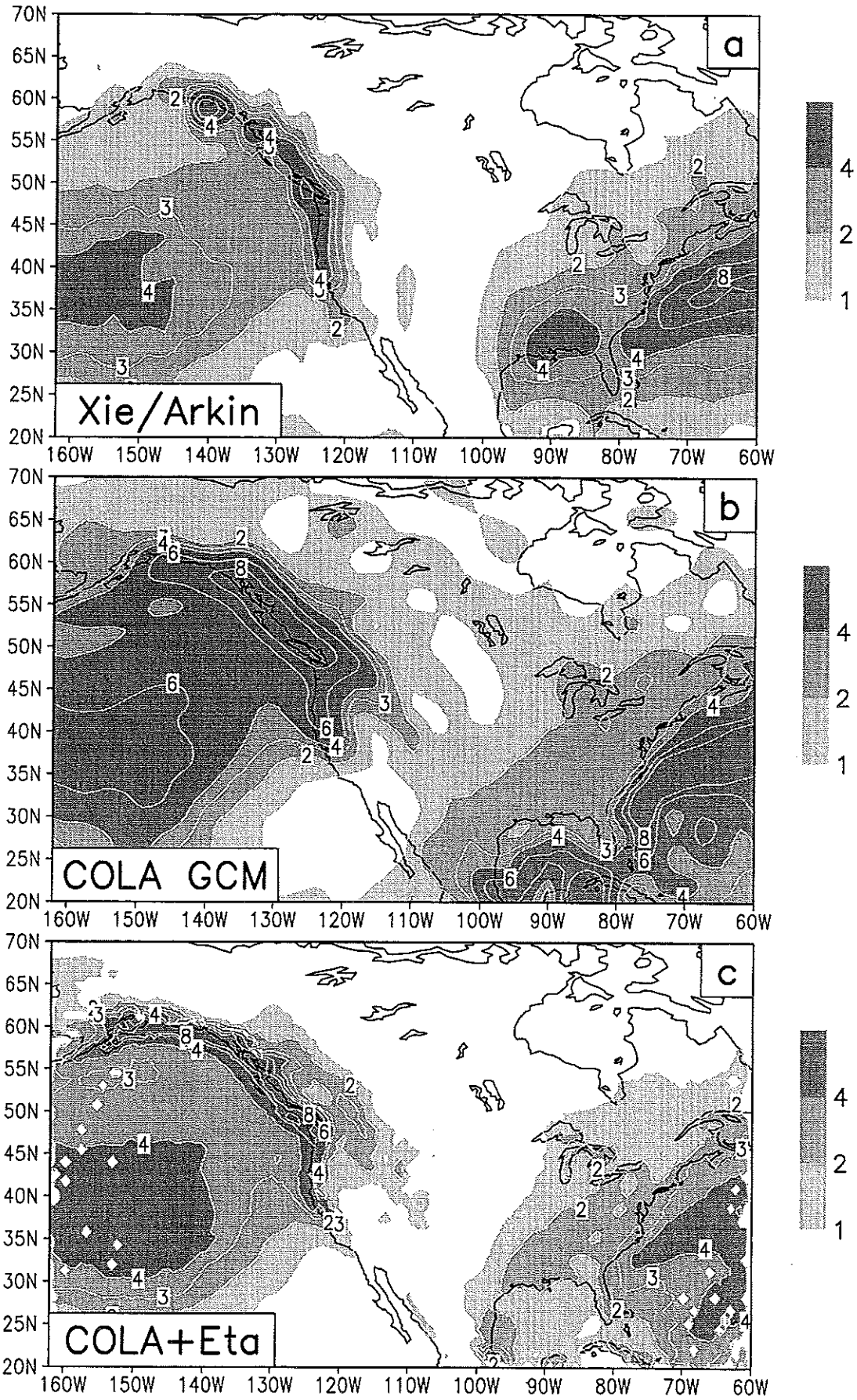
a
Xie/Arkin
b
COLA GCM
c
COLA+Eta
70N
65N
60N
55N
50N
45N
40N
35N
30N
25N
20N
160W
150W
140W
130W
120W
110W
100W
90W
80W
70W
60W
4
2
1

Figure 7

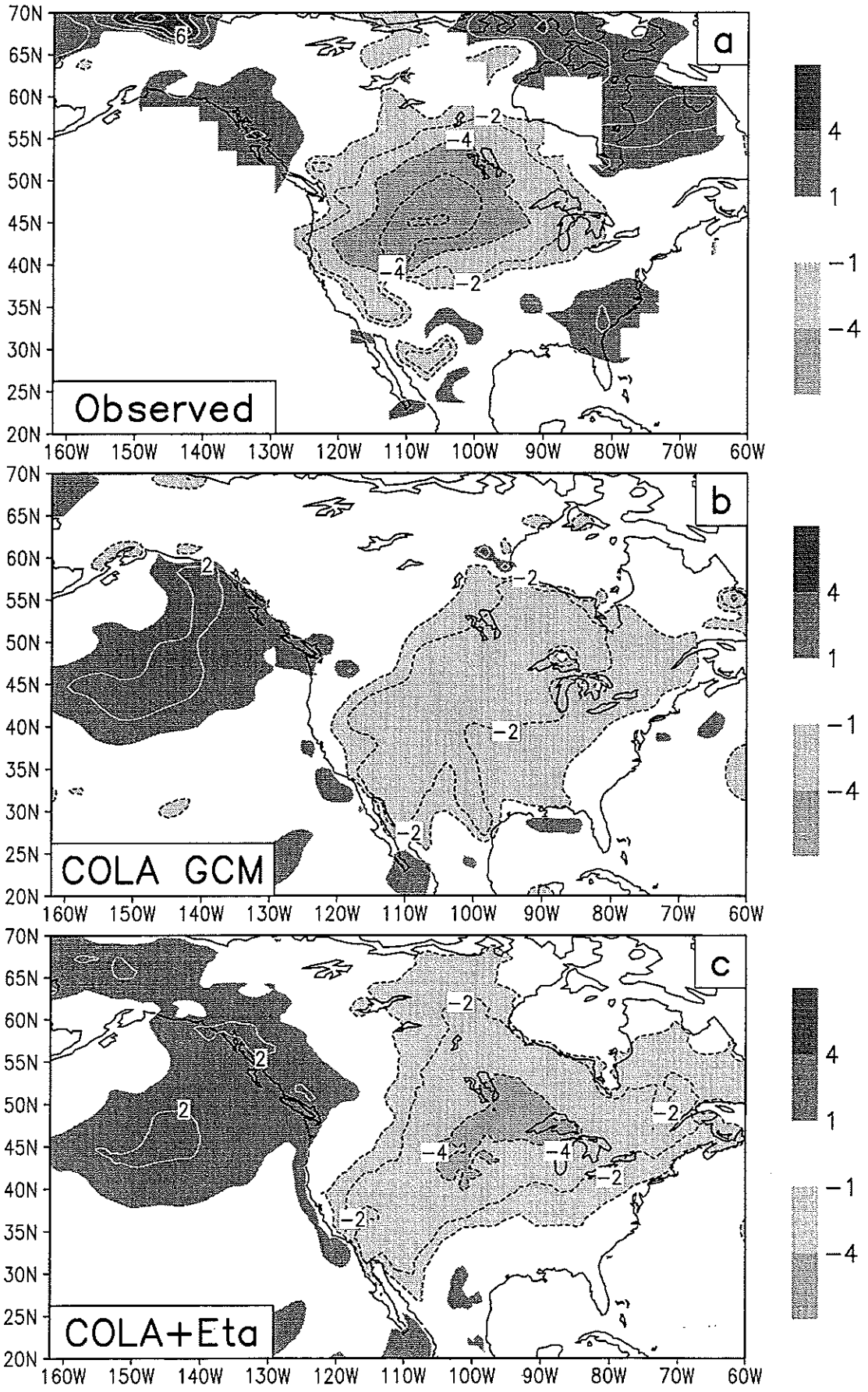
a
Observed
b
COLA GCM
c
COLA+Eta
70N
65N
60N
55N
50N
45N
40N
35N
30N
25N
20N
160W
150W
140W
130W
120W
110W
100W
90W
80W
70W
60W
6
4
2
1
−1
−2
−4

Figure 8

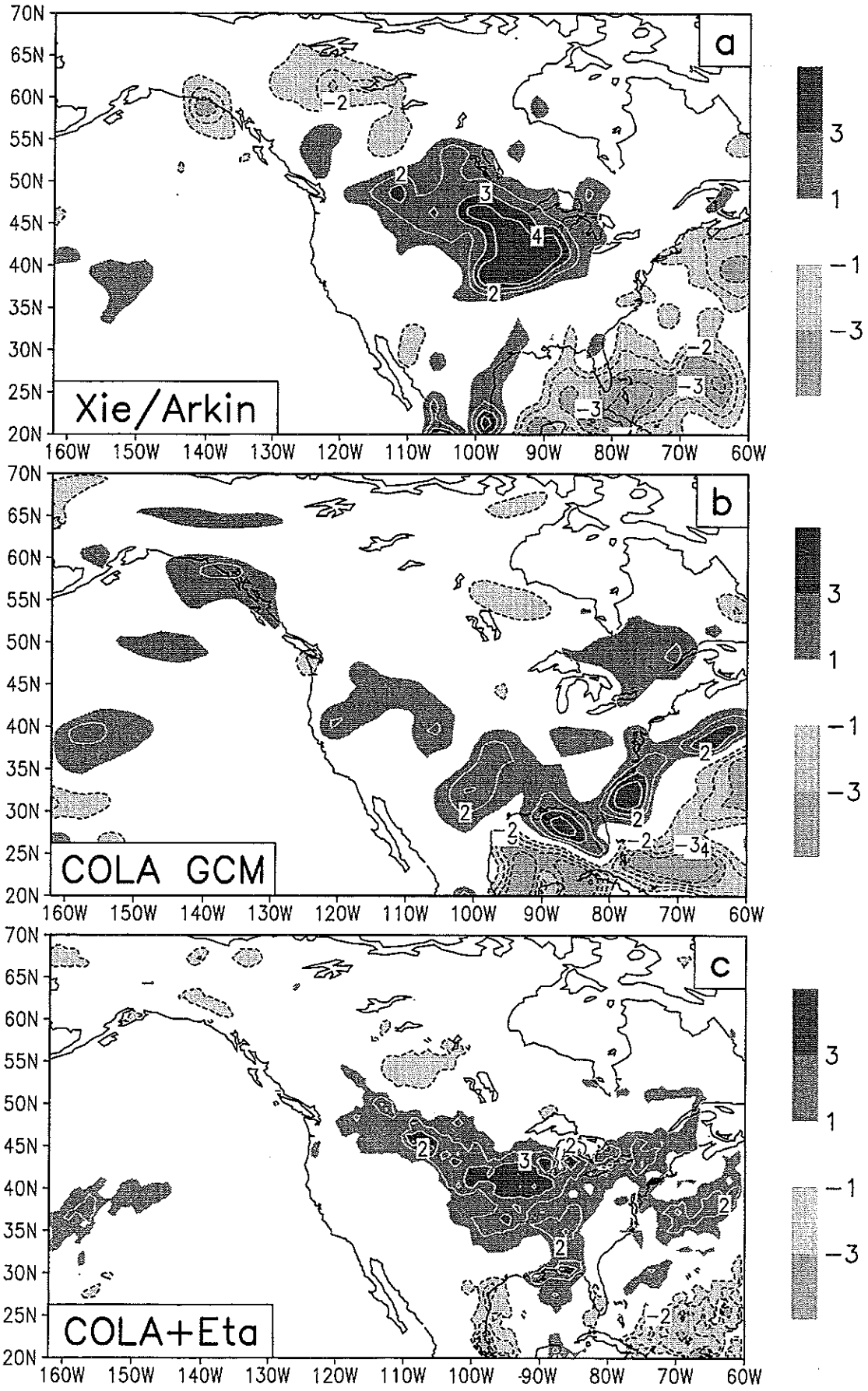
a
Xie/Arkin
b
COLA GCM
c
COLA+Eta
70N
65N
60N
55N
50N
45N
40N
35N
30N
25N
20N
160W
150W
140W
130W
120W
110W
100W
90W
80W
70W
60W
3
1
−1
−3

Figure 9

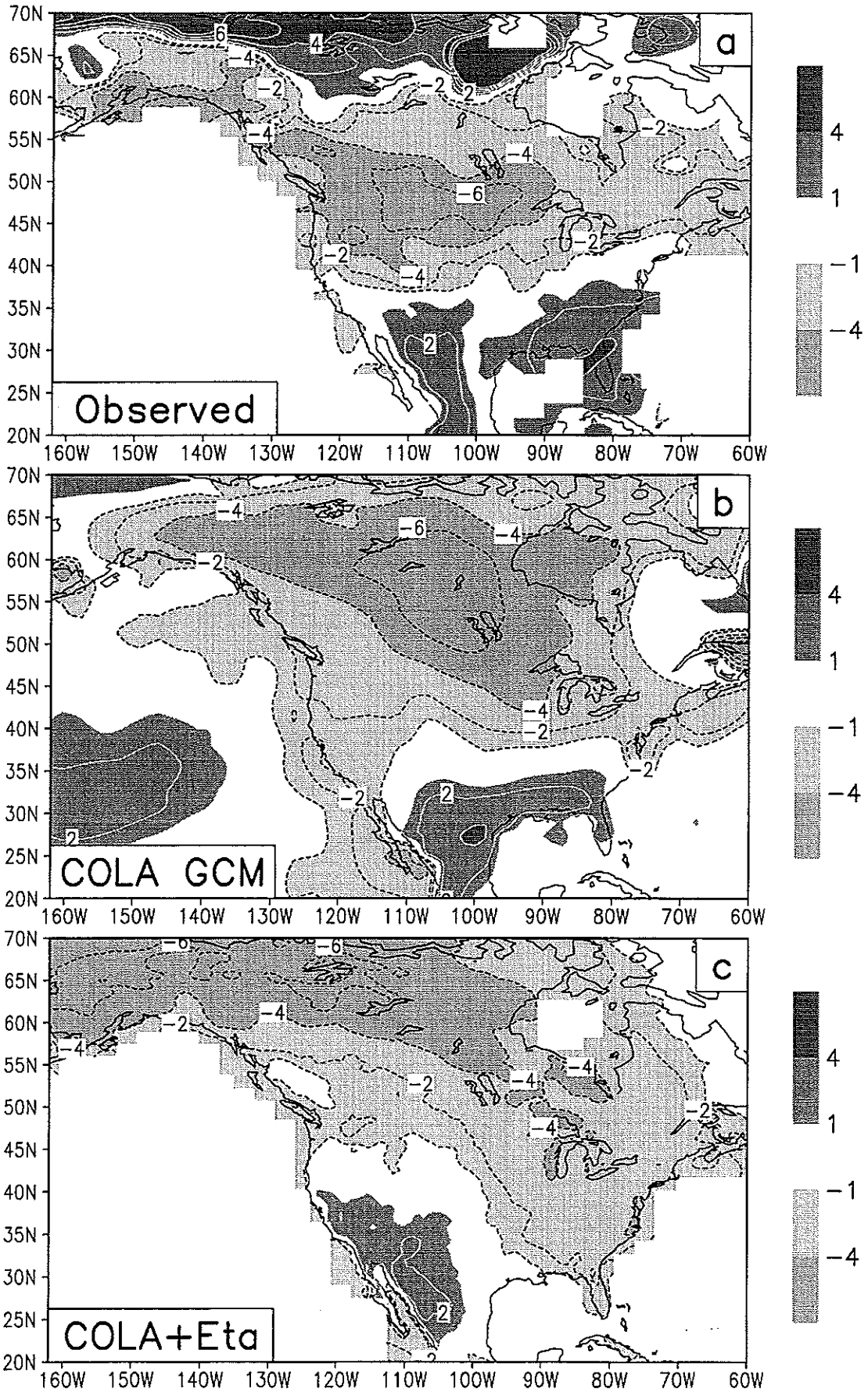
a
Observed
b
COLA GCM
c
COLA+Eta
70N
65N
60N
55N
50N
45N
40N
35N
30N
25N
20N
160W
150W
140W
130W
120W
110W
100W
90W
80W
70W
60W
4
1
−1
−4

Figure 10

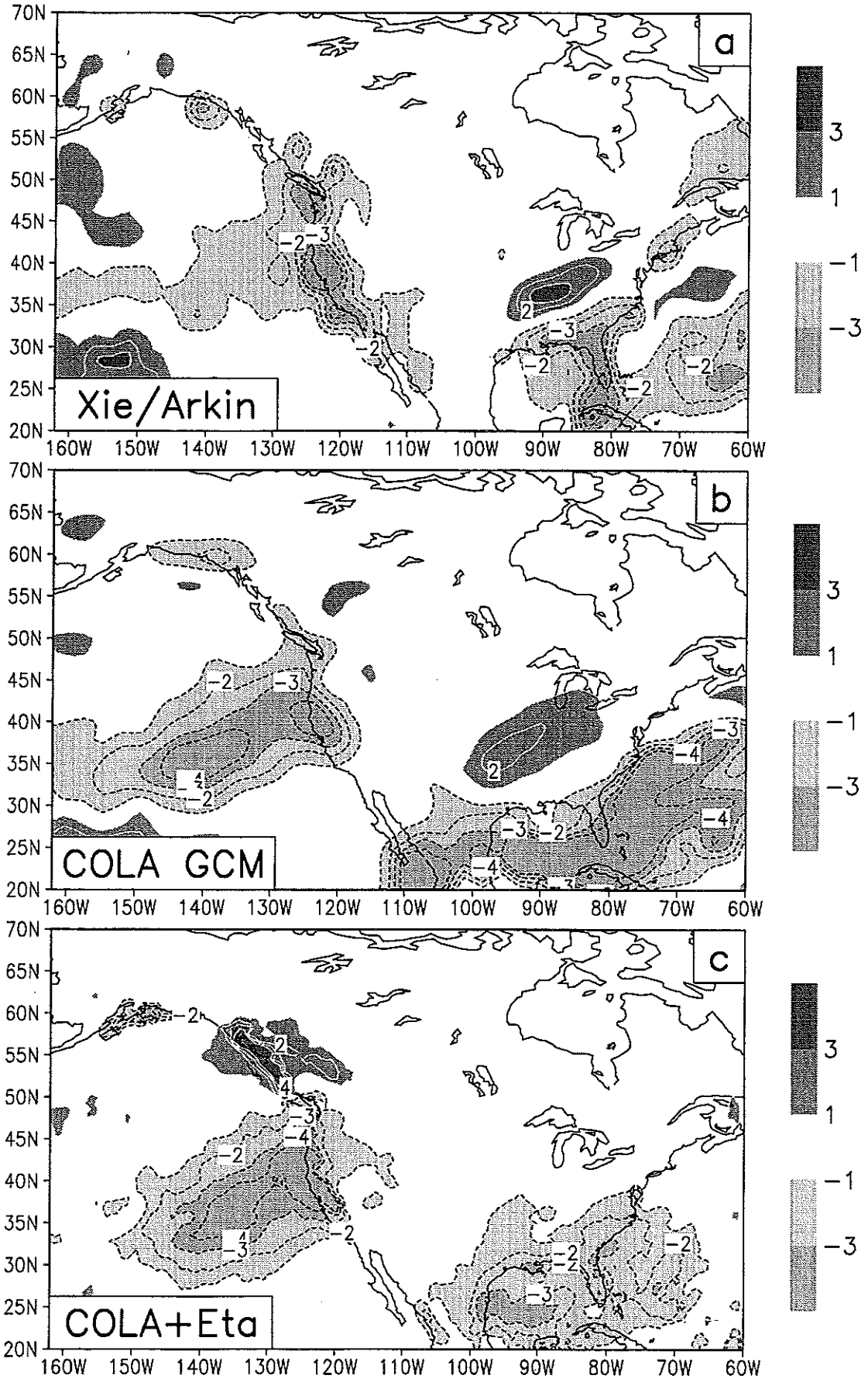
a
Xie/Arkin
b
COLA GCM
c
COLA+Eta
70N
65N
60N
55N
50N
45N
40N
35N
30N
25N
20N
160W
150W
140W
130W
120W
110W
100W
90W
80W
70W
60W
3
1
−1
−3

Figure 11

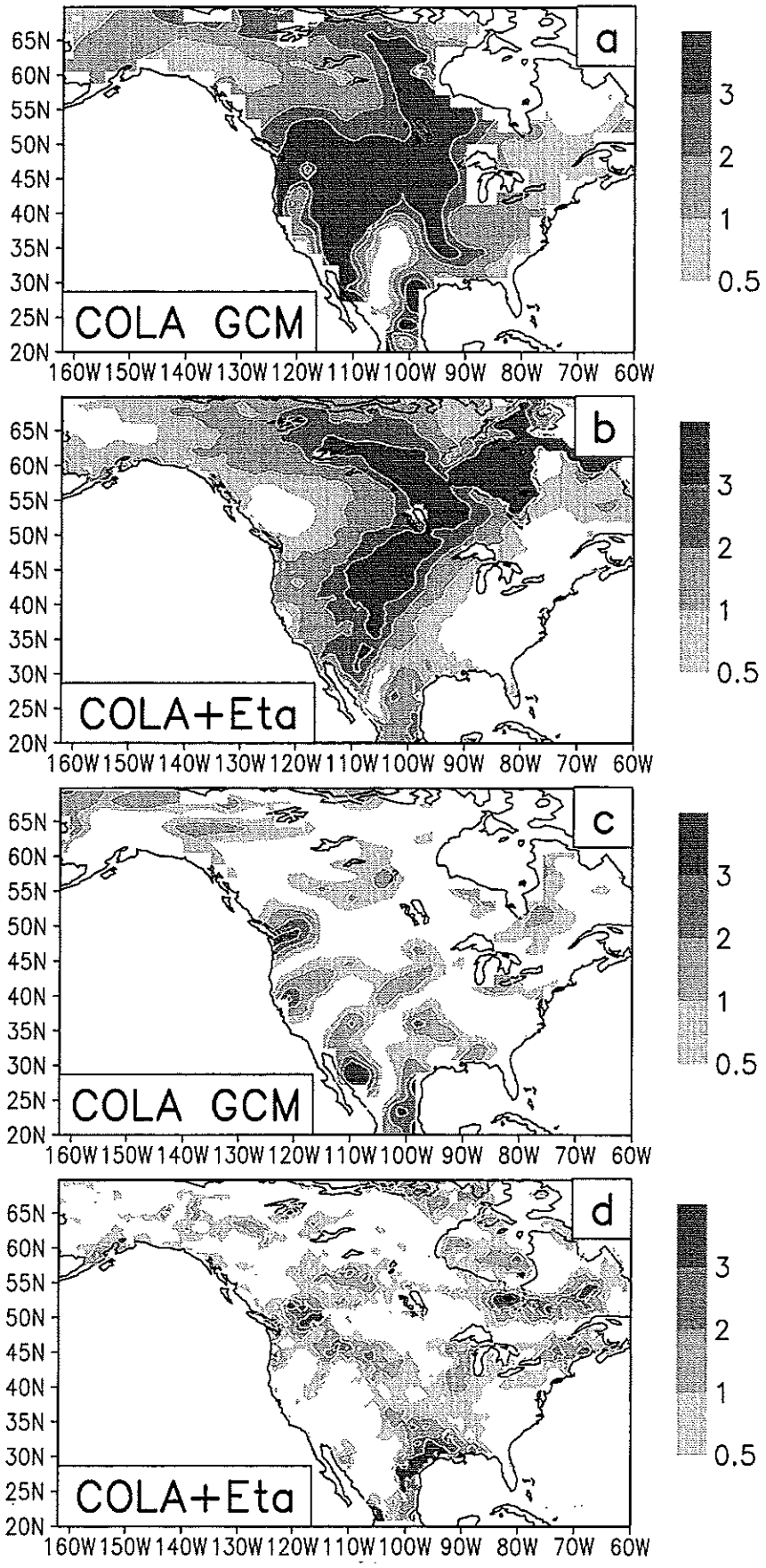
a
COLA GCM
b
COLA+Eta
c
COLA GCM
d
COLA+Eta
65N
60N
55N
50N
45N
40N
35N
30N
25N
20N
160W 150W 140W 130W 120W 110W 100W 90W 80W 70W 60W
3
2
1
0.5

Figure 12

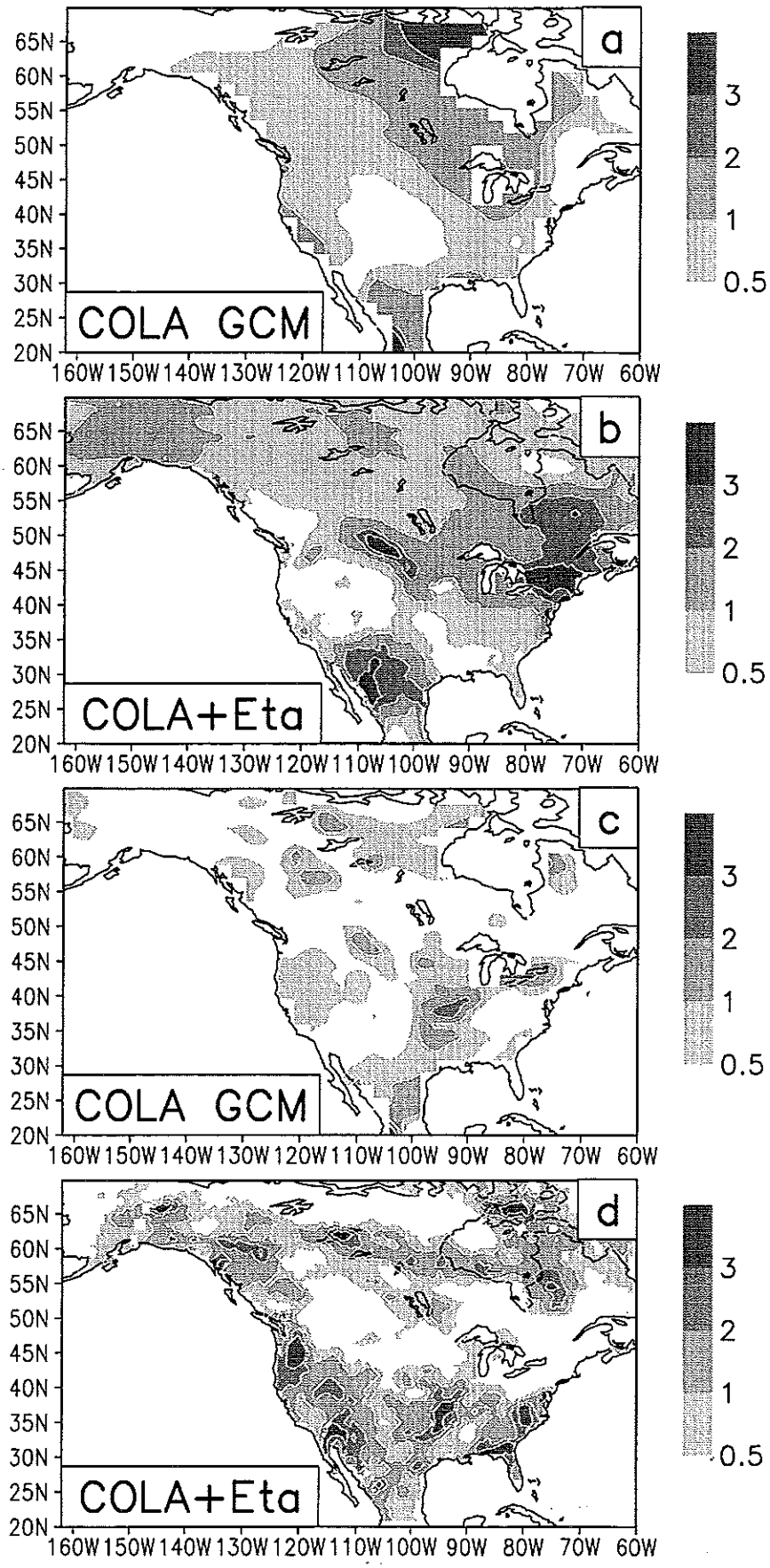
a
COLA GCM
b
COLA+Eta
c
COLA GCM
d
COLA+Eta
65N
60N
55N
50N
45N
40N
35N
30N
25N
20N
160W 150W 140W 130W 120W 110W 100W 90W 80W 70W 60W
3
2
1
0.5

Figure 13

COLA Technical Reports

#1 Ocean Wave Dynamics and El Niño. *E. K. Schneider, B. Huang, & J. Shukla*, April 1994, 46 pp.

#2 Flux Correction and Equilibrium Climate. *E. K. Schneider*, April 1994, 12 pp.

#3 The Effect on Climate of Doubling Deserts. *P. A. Dirmeyer, & J. Shukla*, June 1994, 61 pp.

#4 A Comparison of Two Surface Wind Stress Analyses over the Tropical Atlantic during 1980-1987. *B. Huang, & J. Shukla*, June 1994, 46 pp.

#5 A Pilot Reanalysis Project at COLA. *D. Paolino, Q. Yang, B. Doty, J. L. Kinter III, J. Shukla, & D. Straus*, July 1994, 46 pp.

#6 GCM Simulations of the Life Cycles of the 1988 US Drought and Heatwave. *M. J. Fennessy, J. L. Kinter III, L. Marx, E. K. Schneider, P. J. Sellers, & J. Shukla*, July 1994, 68 pp.

#7 Land-Sea Geometry and its Effect on Monsoon Circulations. *P. A. Dirmeyer*, August 1994, 39 pp.

#8 The response of an Ocean GCM to Surface Wind Stress Produced by an Atmospheric *GCM. B. Huang, & E. K. Schneider*, September 1994, 56 pp.

#9 Meeting on Problems in Initializing Soil Wetness: Review. *P. A. Dirmeyer*, January 1995, 33pp.

#10 Experimental Multi-Season ENSO Predictions with an Anomaly Coupled General Circulation Model. *Z. Zhu and E. K. Schneider*, May 1995, 28pp.

#11 The Impact of Desertification in the Mongolian and the Inner Mongolian Grassland on the East Asian Monsoon. *Yongkang Xue*, May 1995, 50pp.

#12 Annual Cycle and ENSO in a Coupled Ocean-Atmosphere Model. *Edwin K. Schneider, Zhengxin Zhu, Benjamin S. Giese, Bohua Huang, Ben P. Kirtman, J. Shukla, James A. Carton*, May 1995, 57pp.

#13 Improvement in Stratosphere and Upper-Troposphere Simulation with a Hybrid Isentropic-Sigma Coordinate GCM. *Zhengxin Zhu and Edwin K. Schneider*, June 1995, 45pp.

#14 Factors Determining the Precipitation Distribution and Low-Level Flow in the Tropics of an Atmospheric General Circulation Model: Diagnostic Studies. *David G. DeWitt, Edwin K. Schneider, and Anandu D. Vernekar*, June 1995, 56pp.

#15 Multiseasonal Predictions with a Coupled Tropical Ocean Global Atmosphere System. *Ben P. Kirtman, J. Shukla, Bohua Huang, Zhengxin Zhu, and Edwin K. Schneider*, June 1995, 59pp.

#16 An Examination of the AGCM Simulated Surface Wind Stress and Low Level Winds Over the Tropical Pacific Ocean. *Bohua Huang and J. Shukla*, August 1995, 42pp.

#17 Model Based Estimates of Equatorial Pacific Wind Stress. *Ben P. Kirtman, Edwin K. Schneider and Bernard Kirtman*, August 1995, 58pp.

#18 Impact of Vegetation Properties on U.S. Summer Weather Prediction. *Yongkang Xue, Michael J. Fennessy and Piers Sellers*,August 1995, 41pp.

#19 Wave-CISK, The Evaporation-Wind Feedback, and the Intraseasonal Oscillation: Phase Propagation and Scale Selection. *Ben P. Kirtman and Anandu D. Vernekar*,August 1995.

#20 Intercomparison of Atmospheric Model Wind Stress with Three Different Convective Parameterizations: Sensitivity of Tropical Pacific Ocean Simulations. *Ben P. Kirtman and David G. DeWitt,* September 1995, 51 pp.

#21 Variations of Mid-Latitude Transient Dynamics Associated with ENSO. *David M. Straus and J. Shukla,*September 1995, 49 pp.

#22 Tropical Influence on Global Climate. *Edwin K. Schneider, Richard S. Lindzen and Ben P. Kirtman,* February 1996, 29pp.

#23 Precipitation and Water Vapor Transport Simulated by a Hybrid Isentropic-Sigma GCM. *Zhengxin Zhu,*March 1996, 37 pp.

#24 Predictability and Error Growth in a Coupled Ocean-Atmosphere Model. *J. Shukla and Ben P. Kirtman,* March 1996, 11 pp.

#25 Diagnosis of the Mid-Latitude Baroclinic Regime in the NASA DAO Reanalyses and ECMWF Operation Analyses *David M. Straus and Dan Paolino,* March 1996, 48 pp.

#26 Proceedings of the Workshop on Dynamics and Statistics of Secular Climate Variations: Miramare - Trieste, Italy; 4 - 8 December 1995 Editors: *James L. Kinter III and Edwin K. Schneider,* April 1996.

#27 The Effect of Cumulus Convection on the Climate of the COLA General Circulation Model, *David DeWitt,* May 1996, 58pp.

#28 Oceanic Rossby Waves and the ENSO Period in a Coupled Model , *Ben P. Kirtman,* May 1996, 49 pp.

#29 Biosphere Feedback on Regional Climate in Tropical North Africa, *Yongkang Xue,* June 1996.

#30 Characteristics of the Interannual and Decadal Variability in a General Circulation Model, *Bohua Huang and J. Shukla,* July 1996, 55pp.

#31 Scale Dependent Forcings of a General Circulation Model, *David Straus and Yuhong Yi,* July 1996, 34pp.

#32 ENSO Simulation and Prediction with a Hybrid Coupled Model, *Ben P. Kirtman and Stephen E. Zebiak,* August 1996, 50pp.

#33 Seasonal Atmospheric Prediction, *Larry Marx and Michael J. Fennessy,* August 1996, 34pp.

#34 Impact of Initial Soil Wetness on Seasonal Atmospheric Prediction, *Michael J. Fennessy and J. Shukla,* August 1996, 37pp.

#35 The Earth Radiation Budget as Simulated by the COLA GCM, *David G. DeWitt and Edwin K. Schneider,* November 1996, 39pp.

#36 A Note on the Annual Cycle of Sea Surface Temperature at the Equator, *Edwin K. Schneider,* December 1996, 16pp.

#37 Sensitivity of the Simulated Annual Cycle of Sea Surface Temperature in the Equatorial Pacific to Sunlight Penetration. *Edwin K. Schneider and Zhengxin Zhu,* March 1997, 37pp.

#38 A Global Ocean Data Analysis for 1986-1992. *Bohua Huang and James L. Kinter III,* March 1997, 62pp.

#39 ENSO Hindcasts with a Coupled GCM. *Edwin Schneider, Zhengxin Zhu, David DeWitt, Bohua Huang, and Ben Kirtman,* April 1997, 40pp.

#40 GCM Simulations of Intraseasonal Variability in the Indian Summer Monsoon. *R. Krishnan and M.J. Fennessy,* April 1997, 54pp.

#41 Model Simulation of the Influence of Global SST Anomalies on the Sahel Rainfall. *Yongkang Xue and Jagadish Shukla*, April 1997, 25pp.

#42 Predicting Wintertime Skill from Ensemble Characteristics in the NCEP Medium Range Forecasts over North America. *Paul A. Dirmeyer, Brian E. Doty and James L. Kinter III*, April 1997, 31pp.

#43 Decadal Variability in ENSO Predictability and Prediction. *Ben P. Kirtman and Paul S. Schopf*, May 1997, 43pp.

#44 Simulations of the Climate with a Coupled Ocean-Atmosphere General Circulation Model: Seasonal Cycle and Adjustment to Mean Climate. *David G. DeWitt and Edwin K. Schneider*, July 1997, 64pp.

#45 Upper Tropospheric Water Vapor and Climate Sensitivity. *Edwin K. Schneider, Ben P. Kirtman and Richard S. Lindzen*, August 1997, 40pp.

#46 A Broad Scale Circulation Index for the Interannual Variability of the Indian Summer Monsoon. *B.N. Goswami, V. Krishnamurthy, and H. Annamalai*, September 1997, 52pp.

#47 Assessing GCM Sensitivity to Soil Wetness Using GSWP Data, *Paul A. Dirmeyer*, September 1997, 26pp.

#48 A Two Dimensional Implementation of the Simple Biosphere (SiB) Model, *Paul A. Dirmeyer and Fanrong Zeng*, September 1997, 30pp.

#49 Using SST Anomalies to Predict Flood and Drought Conditions for the Caribbean, *A. Chen, A. Roy, J. McTavish, M. Taylor and L. Marx*, September 1997, 41pp.

#50 A Forecast of Precipitation and Surface Air Temperature in North America for Winter (JFM) 1998, *J. Shukla, Dan Paolino, Ben Kirtman, David DeWitt, Paul Dirmeyer, Brian Doty, Mike Fennessy, Bohua Huang, James Kinter, Larry Marx, Edwin Schneider, David Straus, Z. Zhu*, September 1997, 14pp.

#51 The COLA Atmosphere-Biosphere General Circulation Model Volume 1: Formulation, *James L. Kinter III, David DeWitt, Paul A. Dirmeyer, Michael J. Fennessy, Ben P. Kirtman, Larry Marx, Edwin K. Schneider, J. Shukla and David Straus*, October 1997, 46pp.

#52 Climatology and Interannual Variability of Northern Hemisphere Snow Cover and Depth Based on Satellite Observations, *A.S. Bamzai and J.L. Kinter III*, November 1997, 48pp.

#53 Relation Between Eurasian Snow Cover, Snow Depth and the Indian Summer Monsoon: An Observational Study, *A. Bamzai and J. Shukla*, February 1998, 42pp.

#54 Influence of the Indian Summer Monsoon on ENSO, *B. Kirtman and J. Shukla* , May 1998, 52pp.

#55 A Fundamental Limitation of Markov Models, *T. DelSole*, May 1998, 32pp.

#56 The Tropical Ocean Response to a Change in Orbital Forcing, *D. DeWitt and E.K. Schneider*, July 1998, 55pp.

#57 Modeling the Effects of Vegetation on Mediterranean Climate During the Roman Classical Period Part I: Climate History and Model Sensitivity, *O. Reale and P. Dirmeyer*, August 1998, 47pp.

#58 Modeling the Effects of Vegetation on Mediterranean Climate During the Roman Classical Period Part II: Climate History and Model Simulation, *O. Reale and J. Shukla*, August 1998, 68pp.

#59 A Dissipation Integral with Application to Ocean Diffusivities and Structure, *E. Schneider and U. Bhatt*, September 1998, 37pp.

#60 Geophysical Turbulence in the Reanalyses of ECMWF , *D. Straus and P. Ditlevsen*, October 1998, 50pp.

#61 Simulations of a Boreal Grassland Hydrology at Valdai, Russia: PILPS Phase 2(d) , *C. A. Schlosser and Collaborators*, October 1998, 47pp.

#62 Monsoon-ENSO Relationship on Interdecadal Time Scale , *V. Krishnamurthy and B.N. Goswami*, October 1998, 55pp.

Copies of COLA Reports are available from:

Center for Ocean-Land-Atmosphere Studies
4041 Powder Mill Road, Suite 302
Calverton, MD 20705-3106 USA